Chapter 1.

General Introduction

1.1. Duchenne Muscular Dystrophy

1.1.1. Clinical phenotype

Edward Meryon, an English physician, was the first to publish on an inherited disorder we now refer to as Duchenne muscular dystrophy (DMD). In 1852, he described the clinical manifestations of eight affected boys from three families in great detail (Meryon 1852). At the time, Meryon already observed that the progressive muscle wasting and weakness was restricted to muscle and did not affect the nervous system. The disorder was later named after Guillaume Benjamin Amand Duchenne who was the first to study DMD patient biopsies (Duchenne 1868).

Muscle fibers of DMD patients are vulnerable to exercised-induced damage and despite efforts to regenerate, muscle mass is gradually lost resulting in progressive muscle weakness. In DMD patients, the first symptoms become apparent between the age of two and five years and consist of pseudohypertrophy of the calf muscles and difficulties in running, jumping and climbing stairs. Eventually, patients lose muscle coordination, have difficulties walking and rise from the ground by using their arms to climb up their body, which is known as Gower's sign (Gowers 1879). Early in the second decade, patients become wheelchair dependent due to loss of strength in the lower limb muscles. Subsequently, progressive weakness of the shoulder girdle and arms results in loss of function in all extremities (Blake et al. 2002).

Also the heart is affected in more than 90% of the DMD patients. Cardiac involvement is already found in 25% of patients under the age of six. This is recognizable by minor electrocardiographic (ECG) and echocardiographic signs, in the absence of symptoms. Clinical cardiomyopathy is observed from the age of 10 onwards and is first characterized by myocardial hypertrophy in which the interventricular septum is thickened followed by dysrhythmias. Infiltration of fibrotic tissue starts at the left ventricular wall and progressively spreads throughout both ventricles. It eventually results in cardiomyopathy in which chambers are dilated and ventricles have poor contractility resulting in a decreased ejection fraction. The left ventricular posterobasal and lateral walls are predominantly affected (Finsterer and Stollberger 2003).

Patients also develop thoracolumbar scoliosis, for which they can undergo spinal stabilisation surgery (Eagle et al. 2007;Kohler et al. 2005). This deformity of the spinal cord is thought to result from asymmetric weakening of the muscles that support the spinal column (Oda et al. 1993). In the late teens, they develop respiratory impairment and need assisted ventilation first primarily at night, but in more advanced stages in a chronic manner (Lo Mauro et al. 2010). With smooth muscles being affected as well, DMD patients often suffer from bloating, feeling of fullness and constipation (Borrelli et al. 2005). Also cases of acute gastric dilatation and intestinal pseudo-obstruction have been reported. As a consequence of their immobility, body composition is altered with a low bone mineral density, lower lean tissue and higher fat mass compared to healthy age-matched boys. At the age of 13, 44-54% of DMD patients become obese, but the same percentage of boys is underfed when they are 18 years old, primarily resulting from swallowing difficulties (Martigne et al. 2011).

The function of the retina is affected as well. Especially boys that lack the dystrophin isoform Dp260 (see below) often have difficulties in red-green discrimination (Pillers et al. 1999;Costa et al. 2007). The average IQ is one standard deviation below the mean and 20% of the patients have an IQ of less than 70. Learning disabilities, involving dyslexia and dyscalculia are common. However these non-muscle related symptoms are not of a progressive nature (Billard et al. 1992;Emery 1993).

Although improved health care has increased the life expectancy in the Western world, most DMD patients die in their third or fourth decade due to heart or respiratory problems (Eagle et al. 2007).

1.1.2. The *DMD* gene and dystrophin

With an incidence of 1 in 3500 newborn boys, DMD is the most common inherited neuromuscular disorder. It is caused by mutations in the *DMD* gene which is located on the short arm of the X-chromosome (Xp21). It is the biggest known human gene (2.4 Mb) and is also extremely large in other organisms like the mouse, zebra fish and drosophila. The majority of the gene consists of intronic regions, since the coding sequence, ~14 kb spread over 79 exons, only accounts for 0.6% in man (Koenig et al. 1987;Muntoni et al. 2003;Roberts et al. 1993).

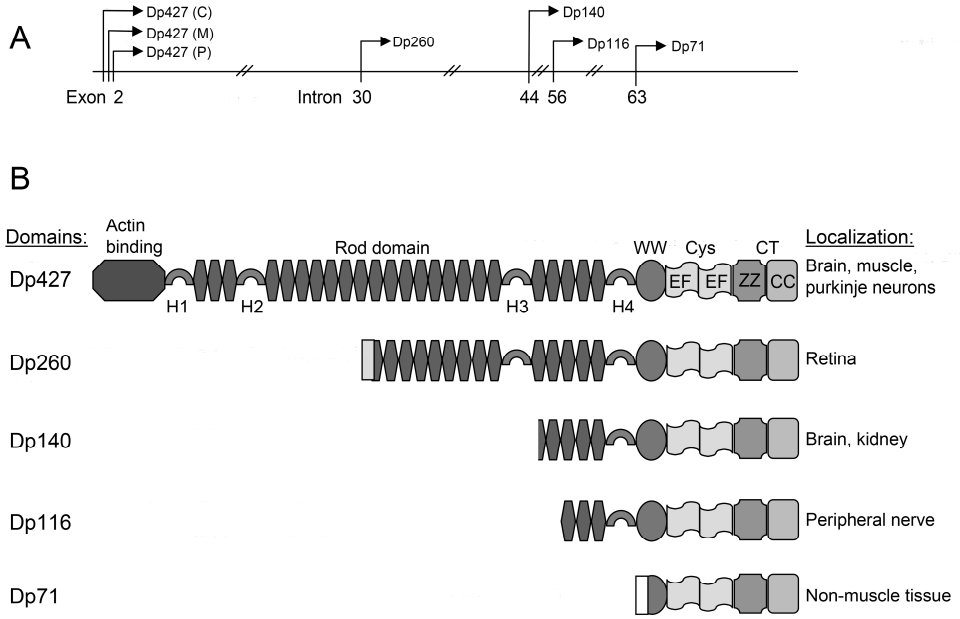

Figure 1. Schematic overview of the different dystrophin isoforms.
A. Five different promoters spread throughout the *DMD* gene ensure transcription of seven dystrophin isoforms; three full-length and four shorter proteins. **B**. Full-length dystrophin is composed of an actin-binding domain, four hinge sites (H1-4), a central rod domain, a WW domain, a cysteine-rich domain (consisting of 15 cysteines, two EF hand motifs and a ZZ domain) and a C-terminal domain (consisting of two coiled coil-domains). None of the smaller isoforms contains the N-terminal actin-binding domain and most lack great parts of the central rod domain. Dp71 even lacks the central rod domain entirely (Figure is based on Willmann et al. NMD 2009).

The *DMD* gene codes for the protein dystrophin of which different isoforms are expressed in several tissues. The isoforms originate from seven promoters spread along the gene (Figure 1). Full-length dystrophin is synthesized from three promoters located before the common exon 2. The isoforms are named after the molecular weight of the protein and the tissue of origin. The Dp427m isoform is synthesized in skeletal and cardiac muscle (Gorecki et al. 1992;Muntoni et al. 2003). The cortical neurons and the hippocampus of the brain synthesize Dp427c, while Dp427p is found in cerebellar Purkinje cells and in lower levels in skeletal muscle. Full-length 427m

dystrophin consists of 3685 amino acids. It takes approximately 12 hours to transcribe 1,770 kb, extrapolating to a transcription time of ~16 hours for the entire gene (Tennyson et al. 1995). It is expressed in very low levels in muscle (0.002% of total muscle protein). Full-length dystrophin contains four domains (Koenig et al. 1988). The N-terminal actin-binding domain is the first distinctive domain. This domain contains two actin-binding sites and facilitates binding of dystrophin to filamentous actin (F-actin) in the subsarcolemmal cytoskeleton. This domain is followed by the central rod domain which consists of 24 triple-helical repeats making it the largest domain. These repeats are interspersed by 4 proline-rich hinge regions (H1-4) (Koenig and Kunkel 1990). The rod domain provides flexibility and elasticity to the protein.

An additional actin-binding domain is located between repeat unit 11-17 (Rybakova et al. 1996) and a neuronal nitric oxide synthase (nNOS) binding domain is present in repeat unit 16-17 (Lai et al. 2009).

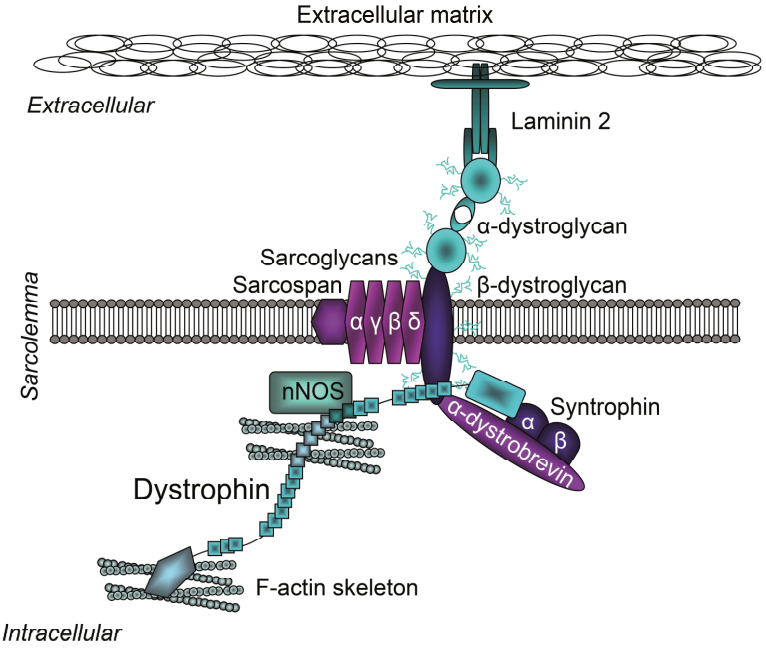

Figure 2. Dystrophin-glycoprotein complex in skeletal muscle.
Dystrophin binds with the N-terminus to the F-actin skeleton of the cell and with the C-terminus to the DGC which is linked to the extracellular matrix. The DGC consists of multiple proteins. Several muscular disorders are caused by the absence of some of these proteins.

The last two domains are the cysteine-rich domain, which includes 15 cysteines, two EF hand motifs and a ZZ domain, and the C-terminal domain that consists of two stretches that form X-helical coiled coil-domains (Koenig et al. 1988). The cysteine-rich domain promotes binding to and localization of the dystrophin-glycoprotein complex (DGC) and contains the domain that binds to β-dystroglycan.

Internal promoters allow the production of four smaller isoforms called Dp260 (retina), Dp140 (brain, kidney, blood vessels and retina), Dp116 (Schwann cells of the peripheral nerves) and Dp71 (most non-muscle tissues). Those proteins lack the actin-binding domain and part of the central rod domain. Dystrophin is located underneath the membrane of muscle fibers, where

the N-terminus binds the intracellular F-actin of the cytoskeleton while the C-terminus connects with the transmembranal DGC that is in turn connected to the extracellular matrix (ECM) (Figure 2). In this way, dystrophin provides stability to muscle fibers during contractions, but it also plays a role in cell signaling. The DGC is a large protein complex that contains, amongst others, sarcoglycans, sarcospan, dystroglycans, syntrophins and dystrobrevins (Ehmsen et al. 2002). Various muscle disorders have been linked to the absence of some of these proteins, where the absence of sarcoglycans or the improper glycosylation of dystroglycans result in various types of Limb girdle muscular dystrophy (Sciandra et al. 2003;Muntoni et al. 2008). In the absence of dystrophin, expression of these proteins is largely reduced and localization at the sarcolemma is lost.

1.1.2.1. The UTRN *gene and utrophin*

In addition to the dystrophin isoforms, also three dystrophin homologues have been described. These share homology with large proportions of dystrophin and are called utrophin (first referred to as dystrophin related protein 1), dystrophin related protein 2 and dystrobrevin. Utrophin is most similar to dystrophin and is the most relevant homologue for the DMD field (Love et al. 1989b). It is transcribed from the *UTRN* gene (0.9Mb) located on chromosome 6 and contains 74 exons. The full length protein is 395kDa and consists of an N-terminal actin-binding domain, a central rod domain, a cysteine-rich and C-terminal domain (Figure 3). Compared to dystrophin, utrophin lacks repeat units 15 and 19 and hinge regions 1 and 3 (Blake et al. 2002;Winder et al. 1995).

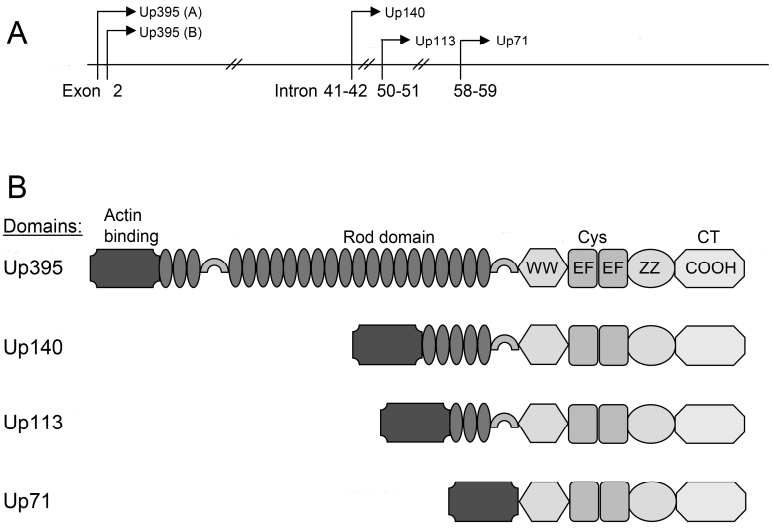

Figure 3. Utrophin isoforms.
A. Representation of the *UTRN* gene with two different promoters giving rise to full-length utrophin A and B, which are expressed at the neuromuscular junction and in vascular endothelial cells respectively. Downstream of the gene, three additional promoters synthesize shorter isoforms. **B**. Schematic representation of full-length utrophin and the three shorter isoforms. The protein structure of full-length utrophin is largely identical to that of dystrophin (Figure design is based on Willmann et al. NMD 2009).

Full-length utrophin is transcribed from two independent promoters; *Utrn-A* and *Utrn-B*, resulting in distinct proteins that differ at the initial 5' ends and in localization as utrophin A is expressed at the neuromuscular junction (NMJ) while utrophin B is expressed at the vascular

endothelium. Like dystrophin, utrophin also has three shorter isoforms; Up140, Up113 (G utrophin) and Up71 (Perronnet and Vaillend 2010;Burton et al. 1999;Dennis et al. 1996;Wilson et al. 1999). Similar to how dystrophin links actin to the DGC complex in muscles, utrophin links actin to a DGC-like complex present at the synaptic membrane, which contains agrin, rapsin and acetylcholine receptors (AChRs) in addition to proteins found in the DGC complex found for dystrophin (Figure 4) (Apel et al. 1995;Haenggi and Fritschy 2006). The expression of utrophin and dystrophin at the synaptic membrane does not overlap.

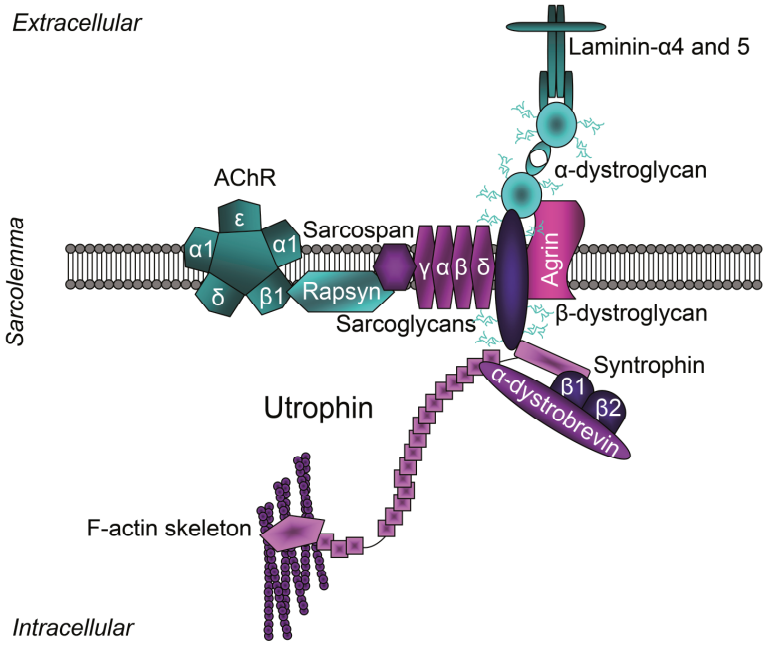

Figure 4. Utrophin-glycoprotein complex at the synaptic membrane.
Utrophin binds with the N-terminus to the F-actin skeleton and with the C-terminus to the DGC. The composition of the synaptic DGC is slightly different from that found at the muscular sarcolemma, e.g. at the synapse, laminin α4 and 5, syntrophin β1 and 2 are expressed whereas laminin α2 and syntrophin α1 and β1 are found at the muscular sarcolemma. Also additional proteins like agrin, rapsyn and the acetylcholine receptors are present at the synaptic membrane.

In heart, utrophin is localized at intercalated discs and microvasculature smooth muscle (Hainsey et al. 2003). During development, in both healthy and DMD foetuses, utrophin A is expressed in developing and regenerating muscle fibers along the entire sarcolemma. In maturing fibers, it is replaced by dystrophin at the sarcolemma and is then solely expressed at the NMJ where it colocalizes with AChRs. It participates in postsynaptic membrane maintenance and AChR clustering (Nguyen et al. 1991;Clerk et al. 1993). In DMD patients and the *mdx* mouse however, overexpression of utrophin A is observed at the sarcolemma in mature muscle fibers compensating for the absence of dystrophin. Although this, to some extent, partially rescues the dystrophic phenotype in mice, overexpression is too low to prevent muscle degeneration in DMD patients. However, the degree in which utrophin is expressed, correlates with disease severity (Kleopa et al. 2006). Mice that lack utrophin (*utrn* $^{-/-}$) but express dystrophin appear healthy and show no muscle pathology, whereas mice that lack both proteins (*mdx/utrn* $^{-/-}$) are very severely affected.

1.1.3. Muscle pathology

In DMD patients, the absence of functional dystrophin leads to a series of events, which finally result in replacement of muscle fibers by fibrotic and fat tissue. The exact cause of initiation of this pathological cascade is not fully understood, but several hypotheses have been proposed to explain why the absence of dystrophin results in vulnerable fibers and degeneration (Figure 5).

As mentioned before, dystrophin links the actin filaments to the DGC, maintains fiber integrity during eccentric contractions and plays a role in signaling. In the absence of dystrophin, muscle contractions result in disruptions of the membrane and thereby increased membrane permeability. The presence of these membrane tears is evident by elevated serum creatine kinase (CK) levels. CK is an enzyme that catalyses the conversion of creatine into phosphocreatine turning adenosine triphosphate (ATP) into adenosine diphosphate (ADP). Muscles consume ATP in large amounts and CK is mainly found in this tissue. Upon fiber damage, CK leaks through tears in the membrane into the bloodstream resulting in very high levels of 20,000 to 50,000 U/L (normal human values <200 U/L) (Emery and Muntoni 2003). This process is known to be exacerbated by exercise. Even in healthy individuals, CK levels are elevated after a bout of strenuous exercise as a consequence of membrane disruptions.

Through the same membrane tears from which CK leaks out of the fibers, extracellular Ca^{2+} passively enters. In addition, Ca^{2+} enters the fibers actively through mechanosensitive stretch-activated (SAC) channels. DMD patients have increased numbers of SAC channels and they are also more active than those in healthy individuals. The increased Ca^{2+} level causes a disruption of the intracellular Ca^{2+} homeostasis (Allen et al. 2010;Deconinck and Dan 2007). The Ca^{2+} also activates proteases like calpain, which degrade a wide range of skeletal muscle proteins, causing more membrane damage and also activate the SAC channels further, enabling more Ca^{2+} to enter and thereby creating a feedback loop of Ca^{2+} entering the fiber, eventually resulting in fiber death. To some extent, excessive intracellular Ca^{2+} will be taken up by mitochondria (Blake et al. 2002;Chen et al. 2000). However, due to the chronic nature of the disease, mitochondria get structurally damaged, inducing the downregulation of several important genes. This results in malfunction of mitochondria, leading to impaired oxidative phosphorylation and thereby a loss of energy. In addition, damaged mitochondria cause reactive oxygen species (ROS), produced by inflammatory cells like neutrophils and macrophages (Whitehead et al. 2006). ROS promote activation of transcription factor nuclear factor NF-κB, which regulates the expression of pro-inflammatory cytokines like TNF-α and Interleukine (IL)-1B. NF-κB itself inhibits muscle cell differentiation and thus the regeneration process. ROS levels are further increased via a positive feedback loop in which TNF-α exacerbates inflammation. The elevated ROS levels can be scavenged by nitric oxide (NO). NO is formed by nNOS and functions as an endogenous messenger molecule and induces vaso-dilatation. In healthy individuals nNOS is recruited to the membrane by dystrophin. In DMD patients, the absence of dystrophin results in de-localization of nNOS, forcing it to freely float in the cytoplasm (Lai et al. 2009). Since nNOS levels are decreased in DMD patients, NO levels are also largely reduced which disallows fibers to decrease ROS levels and thereby exacerbates continuous fiber damage by ROS.

The pathological cascade initiated by disrupted calcium homeostasis eventually results in fiber necrosis, which induces a chronic inflammatory response that triggers fibrosis. The immune response consists of numerous components including leukocyte adhesion, chemokine signaling, diapedesis, invasive cell type specific markers and complement system activation. The inflammatory cells produce cytokines and other toxins that further damage the muscle fibers.

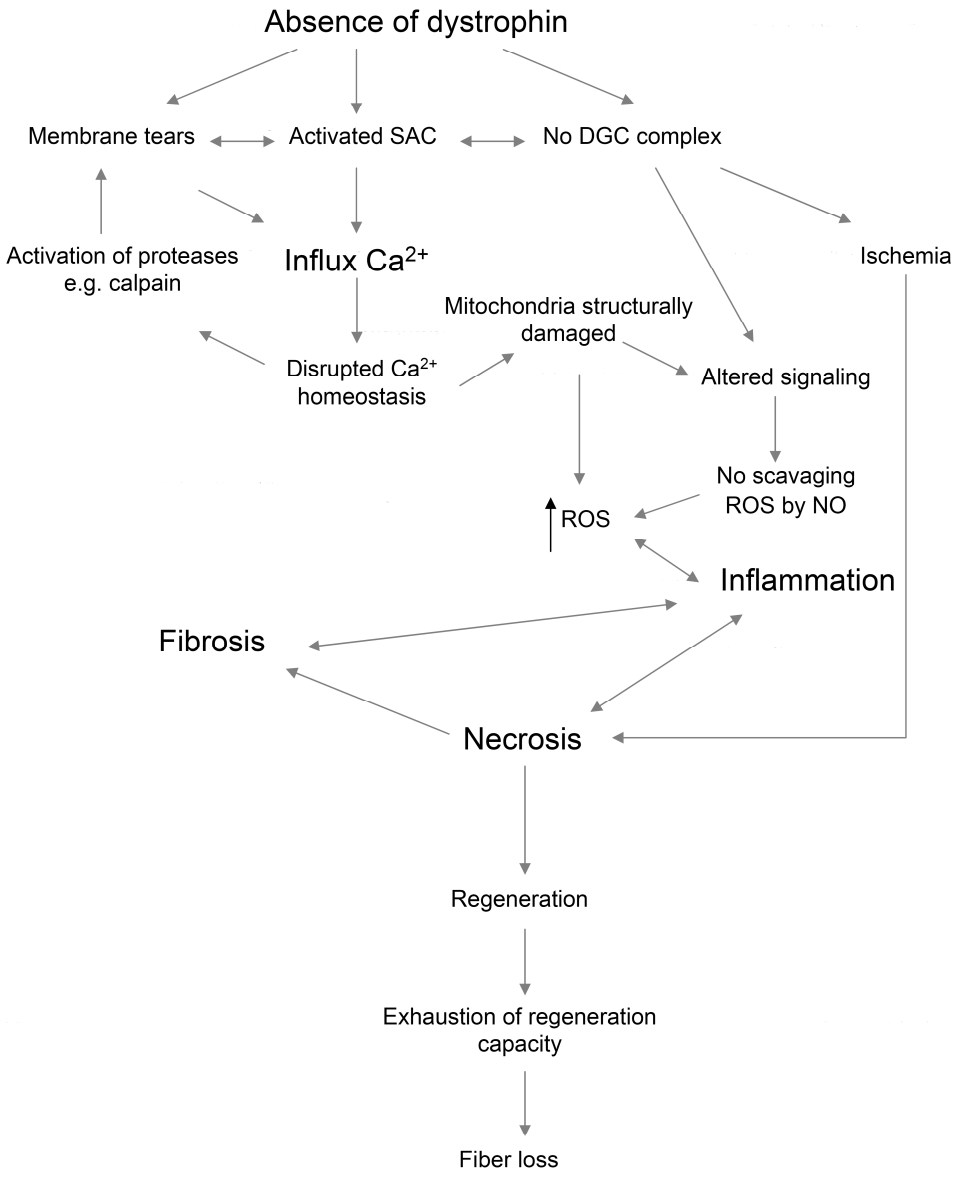

Figure 5. Schematic overview of pathogenesis in skeletal muscles of DMD patients.
In absence of dystrophin an extensive cascade of pathological events is chronically triggered that eventually results in the replacement of muscle fibers by connective and fat tissue leading to loss of muscle function.

Blood vessel abnormalities, including impaired vasodilatation resulting from low NO levels, have been reported in DMD patients. Especially during exercise, when the need of oxygen is higher, muscle ischemia may occur (Miike et al. 1987;Saito et al. 2005;Sander et al. 2000). In skeletal muscle, degenerated fibers are replaced through regeneration. This does not occur in heart as cardiomyocytes do not contain satellite cells (Blake et al. 2002;Deconinck and Dan 2007).

Regenerated fibers are characterized by central nucleation which originates from the differentiation and fusion process of myoblasts into myotubes. Additionally, to compensate for the loss of force-generating capacity, muscles increase in mass by undergoing hypertrophy (Karpati et al. 1988;Narita and Yorifuji 1999). Upon exhaustion of the regenerative capacity, fibers are gradually replaced by connective and adipose tissue. With decreased numbers of muscle fibers from which CK leaks out, serum CK levels drop. The described pathological hallmarks are clearly visible in DMD patient biopsies, which contain groups of necrotic or degenerated fibers, fibrotic and fatty tissue.

Although muscle sections of DMD patients are essentially dystrophin negative, in about 50% of patients ~1-10% of the fibers express some dystrophin. Those so-called 'revertant' fibers express dystrophins that can lack up to 30 exons of the rod-domain in mice. Revertant fibers originate most probably from secondary mutations which re-frame the transcript enabling synthesis of truncated but functional dystrophin (somatic reversion). It is hypothesized that this happens in a specific subset of myogenic stem cells that proliferate in response to degeneration. Revertant fibers are most often found in small clusters and have the same deletion within a cluster, while this often differs per cluster. This indicates that fibers within a cluster inherit the secondary mutation from the same myogenic stem cells (Hoffman et al. 1990;Thanh et al. 1995;Klein et al. 1992).

The degree in which individual skeletal muscles and the heart are affected differs. Some muscles like the diaphragm are severely affected, while others like the soleus are partly spared. Extraocular muscles even appear to entirely escape from the pathological events. Also the order in which muscles are affected and fibrosis and fatty tissue infiltrations are observed is chronological (Torriani et al. 2011;Marden et al. 2005). The exact cause(s) for both phenomena are unclear, however several hypotheses exists. Most often, severely affected muscles are the ones that are constantly used and therefore undergo more stress than those which are rarely used. As exercise exacerbates disruption of the intracellular Ca^{2+} homeostasis this might underlie differences in severity. However, although the soleus is often used during movements, it is largely protected from pathology. It has been hypothesized that this muscle is spared until late in the disease because it mainly consists of slow muscle fibers.

Individual fibers contain functionally distinct isoforms of myosin heavy chain (MyHC) (Gregorevic et al. 2008). Based on the different MyHC isoforms, several fiber types have been identified, which differ in their functional properties. There are two types of muscle fibers. Slow twitch (type I) fibers are efficient at using oxygen (aerobic) and therefore stand muscle contraction over a long time. Fast twitch (type II) fibers use glycogen (anaerobic) and are better at generating short bursts of strength than slow muscles, however they fatigue quicker. Type II fibers can be further grouped into type IIa, IIb and IId/x fibers (Schiaffino et al. 1989). Type IIa fibers are intermediate fast twitch fibers that can use both an aerobic and anaerobic metabolism for energy supply, making them more a combination of type I and II fibers. Type IIb and IId/x fibers only use an anaerobic metabolism. Type II fibers have a larger diameter than type I fibers and are subjected to the greatest mechanical stress during muscle contraction. Most often muscles containing primarily fast fibers are more vulnerable to mechanical damage and earlier affected than muscles that mainly consist of slow fibers (Table 1). Muscles can primarily consist of slow or fast fibers or of a mixture of both types. Depending on the demand of muscles, fiber type compositions can change over time, which happens in a distinct order: type IIb → type IId/x → type IIa → type I. Exercise-induced fiber type switches have been described in mice, as well as differences in composition between mouse strains that differed in disease severity.

Muscle	Fiber type composition	Severity pathology
Quadriceps	Mixed	Moderate
Gastrocnemius	Mixed	Moderate
Tibialis anterior	Fast	Moderate
Soleus	Slow	Mild
EDL	Fast	Moderate
Triceps	Mixed	Moderate
Biceps	Mixed	Moderate
Diaphragm	Fast	Severe

Table 1. Overview of fiber type composition and the degree of histopathology.
The table is based on several studies in *mdx* mice of which fiber type composition of several muscles was determined. Fiber types and the timing of onset of pathological symptoms closely correlate, however multiple other factors play a role as well (Table is adapted from Willmann et al NMD 2012).

In healthy muscle, individual fibers express only one MyHC isoform. Expression of multiple different MyHC isoforms is found in dystrophin negative fibers (Willmann et al. 2011;Emery and Muntoni 2003;Johnson et al. 1973;Webster et al. 1988).

However, fiber type composition is not the only factor that influences the order of initiation of muscle pathology (Emery and Muntoni 2003). Other factors are the number of SAC channels per muscles, differences in regeneration capacity, muscle fiber diameter and length, mitochondrial content, growth rate during development and expression levels of utrophin and members of the DGC (Lewis and Ohlendieck 2010;Porter 1998;Grounds and Shavlakadze 2011). Differences in embryonic origin might play a role as well as muscles derived from the somatic mesoderm are more severely affected than those derived from the paraxial mesoderm. It has also been speculated that some muscles have improved ability to regulate Ca^{2+} homeostasis and that they possess mechanical properties that make them more resistant to damage (Khurana et al. 1995;Wiesen et al. 2007). For example the functional properties of extraocular muscles are more advanced as they display faster peak contraction rates, higher fatigue resistance profiles and have smaller motor units which are less prone to damage (Thomas et al. 2008).

1.1.4. Antisense-mediated exon skipping

In order to synthesize dystrophin protein, a pre-mRNA transcript is generated from the *DMD* gene. During splicing, all introns are spliced out and exons joined so that mRNA is formed. This mRNA is used as a template for protein synthesis, where every three consecutive nucleotides contain the information for one amino acid. DMD patients have mutations that disrupt the reading frame, e.g. a deletion of an exon that contains a number of base pairs that is not divisible by three. This leads to a shift in the reading frame, inclusion of aberrant amino acids and generally a premature stop codon (UAA, UGA or UAG) and untimely truncation of protein translation. Since dystrophin forms a flexible bridge-like connection between the intracellular F-actin filaments and the ECM, and only one bridge-head remains in DMD patients, this function is lost, resulting in the previously described pathogenesis.

Mutations that maintain the reading frame in the *DMD* gene lead to Becker muscular dystrophy (BMD) which affects 1:20,000 men (section 1.3.2). In these patients, a shorter, internally deleted, but partly functional protein is synthesized. The bridge-like connection is maintained in these patients (albeit with an altered connecting domain) and proteins of the DGC

are expressed to some extent. These fibers are supposed to be less vulnerable to exercise-induced damage which leads to a less pronounced pathology and better life expectancy. Some of these patients even lack over two thirds of the central rod domain, indicating that large parts of this domain can be missed (England et al. 1990;Love et al. 1989a).

1.1.4.1. The concept of exon skipping

With no causal treatment available for DMD, effort has been put into attempting to restore the disrupted reading frame (Aartsma-Rus 2010). With the use of antisense oligonucleotides (AONs), which are modified, small pieces of DNA or RNA (~6-8 kDa), signals that are required for inclusion of an exon can be hided from the splicing machinery, so that this exon and its flanking introns are spliced out during pre-mRNA splicing. In this way, the reading frame is restored and internally deleted BMD-like dystrophin proteins are synthesized. As shown in the example of Figure 6, a deletion of exon 52 disrupts the reading frame and causes protein synthesis to stop prematurely. With AONs directed to exon 51, this exon will be skipped, thereby restoring the reading frame enabling the synthesis of a BMD like dystrophin protein.

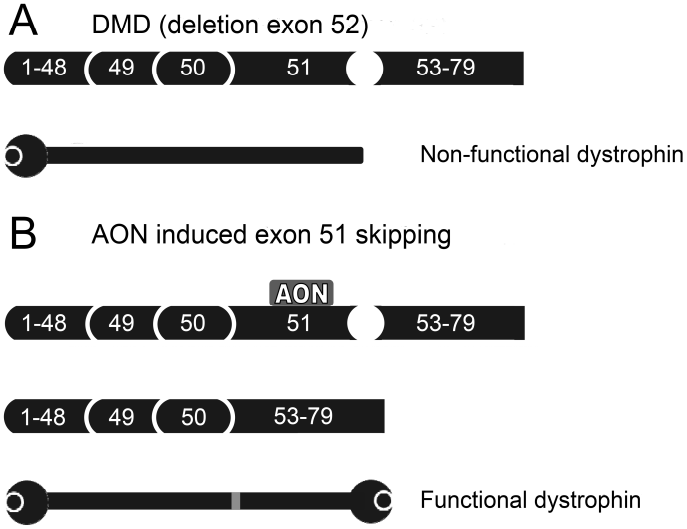

Figure 6. Antisensense oligonucleotide mediated exon 51 skipping.
A. In DMD out-of-frame deletions lead to premature stop codons and truncated, non-functional dystrophins.
B. Using AONs, an exon can be hidden from the splicing machinery, restoring the open reading frame and allowing the production of internally deleted, partly functional dystrophins. The synthesized protein has an unnatural transition (represented by the grey bar) resulting from the lack of the skipped exon (From van Putten et al. Expert Opin. Biol. Ther.).

Mutations found in DMD patients can occur anywhere across the entire gene, but a major hotspot is present between exon 45 and 53 (den Dunnen et al. 1989). Exon skipping is a mutation specific approach, as for different mutations different exons have to be skipped to restore the reading frame. However, skipping of some exons benefits larger groups of patients with different mutations. Exon skipping can be applied to all reading frame disrupting exons of the central rod domain and theoretically might benefit over 90% of the DMD patients. Only a small proportion of all mutations (5-10%) cannot be addressed with this approach. These consist of mutations in the two outer exons; 1 and 79 as these exons cannot be skipped, and mutations

that also result in DMD while they maintain the open reading frame, e.g. mutations that remove either all actin-binding domains or the cysteine-rich domain (Aartsma-Rus et al. 2009).
In the majority (65%) of DMD patients one or more exons are deleted. Here, often skipping one or two flanking exons corrects the reading frame. Skipping two exons, so-called double exon skipping, is feasible by using a combination (cocktail) of AONs targeting the two exons. *In vitro* transfection of patient-derived cell cultures using an AON cocktail to induce double exon skipping results in only slightly lower amounts of dystrophin expressing cells compared to single exon skipping (Aartsma-Rus et al. 2004a).

Figure 7. Overview of the exons of the *DMD* gene.
Light grey bars represent in-frame exons, which can be deleted without disrupting the reading frame. Black exons represent out-of-frame exons and deletions of these exons disrupt the reading frame resulting in DMD. For these exons one or multiple neighbouring exons need to be skipped to restore the reading frame. (Based on Aartsma-Rus et al. Hum. Mut 2008 used with kind permission of John Wiley and Sons).

Small mutations (nonsense mutations, small deletions or insertions and splice site mutations) are found in 28% of the patients. For these patients the reading frame can generally be corrected by only skipping the mutated exon when this is an in-frame exon, or together with an adjacent exon in case of an out-of-frame exon (Figure 7). Duplications, found in 7% of the patients, are more challenging to address with exon skipping (Aartsma-Rus et al. 2007). AONs are sequence specific and cannot distinguish between the original and duplicated exon as they both contain the same sequence. In case of single exon duplications either that exon or the original exon can be skipped to restore the reading frame. However, when skipping efficiency it too high (i.e. close to 100%), both the original and duplicated exon are skipped, which is reading frame disrupting. By skipping an additional exon in addition to the duplication this can sometimes be remedied. The duplication of exon 2 is the most common and makes up 12.7% of all duplications. When the duplication consists of multiple exons, exon skipping becomes very complex and restoration of the reading frame has not been feasible to date for these mutations. Based on data of the Leiden Open Variation Database, it is known that the largest group of patient (13%) would benefit from exon 51 skipping. Therefore skipping this exon is the current focus of clinical development (Aartsma-Rus et al. 2009). As shown in Table 2, 41% of the patients will benefit from AONs skipping 10 exons.

RANKING	EXON(S)	ALL MUTATIONS	DELETIONS SMALL	MUTATIONS SINGLE	EXON DUPLICATIONS
1	51	13.0%	19.1%	0.3%	3.0%
2	45	8.1%	11.8%	0.2%	2.2%
3	53	7.7%	11.4%	0.1%	1.5%
4	44	6.2%	8.8%	0.4%	2.7%
5	46	4.3%	6.2%	0.2%	1.6%
6	52	4.1%	5.7%	0.5%	2.3%
7	50	4.0%	5.6%	0.2%	1.9%
8	43	3.8%	5.3%	0.2%	2.6%
9	6 and 7	3.0%	3.6%	0.1%	6.3%
10	8	2.3%	2.3%		8.0%
11	55	2.0%	2.7%	0.8%	0.2%
12	2	1.9%	1.3%		12.7%
13	69 and 70	1.4%		5.6%	
14	19 and 20	1.1%		4.6%	
15	45 and 51	1.1%	1.7%		
16	58 and 59	1.1%		4.5%	
17	17	1.0%	1.1%	0.1%	3.1%
18	7	1.0%	1.4%		0.8%
19	65 and 66	1.0%		3.9%	
20	43 and 44	0.9%		3.5%	
21	12	0.8%	1.0%	0.3%	1.4%
22	23	0.8%		3.1%	
23	18	0.9%	1.0%	0.1%	2.5%
24	20	0.8%	1.0%	0.2%	1.2%
25	21	0.8%	0.5%	1.2%	1.6%
26	17 and 18	0.8%		3.1%	
27	11 and 12	0.7%		2.9%	
28	68 and 69	0.7%		2.9%	
29	19	0.6%	0.5%	0.4%	1.8%
30	22	0.6%	0.6%	0.1%	1.8%
31	45 and 53	0.6%	0.9%		
32	41	0.6%		2.3%	
33	14	0.6%		2.2%	
34	54 and 55	0.6%		2.2%	
35	20 and 21	0.5%		2.1%	
36	35	0.5%		2.1%	
37	54	0.5%	0.6%		1.0%
38	24	0.5%		2.0%	
39	40	0.5%		2.0%	
40	34	0.4%		1.8%	
41	56	0.4%	0.6%		0.5%
42	11	0.4%	0.3%	0.2%	2.3%
43	16	0.4%		1.7%	
44	39	0.4%		1.7%	
45	62 and 63	0.4%		1.5%	
46	64	0.4%		1.6%	
47	7 and 8	0.4%	0.4%	0.5%	0.2%
48	26	0.4%		1.5%	
49	10	0.4%		1.4%	
50	51 and 52	0.4%		1.4%	
51	6	0.4%	0.3%		1.6%

RANKING	EXON(S)	ALL MUTATIONS	DELETIONS SMALL	MUTATIONS SINGLE	EXON DUPLICATIONS
52	52 and 53	0.3%		1.4%	
53	74	0.3%		1.4%	
54	3	0.3%		1.2%	0.5%
55	13	0.3%		1.3%	
56	21 and 22	0.3%		1.3%	
57	32	0.3%		1.3%	
58	48	0.3%		1.3%	
59	55 and 56	0.3%		1.3%	
60	69	0.3%		1.3%	
61	30	0.3%		1.3%	
62	44 and 45	0.3%		1.3%	
63	47	0.3%		1.1%	0.3%
64	25	0.3%		1.1%	
65	60	0.3%		1.0%	0.3%
66	75 and 76	0.3%		1.2%	
67	5	0.3%		1.0%	
68	27	0.3%		1.0%	
69	50 and 51	0.3%		1.0%	
70	50 and 55	0.3%	0.4%		
71	56 and 57	0.3%		1.0%	
72	57	0.3%	0.2%	0.2%	0.9%
73	28	0.2%		1.0%	
74	4	0.2%		0.9%	
75	29	0.2%		0.9%	
76	38	0.2%		0.7%	0.5%
77	52 and 55	0.2%	0.3%		
78	33	0.2%		0.8%	
79	36	0.2%		0.8%	
80	37	0.2%		0.8%	
81	68	0.2%		0.7%	
82	70	0.2%		0.7%	
83	9	0.2%		0.7%	
84	61	0.2%	0.03%		1.6%
85	15	0.2%			
86	43 and 53	0.2%	0.2%		
87	63	0.1%	0.1%	0.3%	0.2%
88	43 and 51	0.1%	0.2%		
89	59 and 60	0.1%	0.2%		
90	65	0.1%		0.5%	
91	66	0.1%	0.03%	0.4%	
92	6 and 8	0.1%	0.1%	0.2%	
93	45 and 46	0.1%		0.4%	
94	58	0.1%	0.1%	0.1%	0.5%
95	61 and 62	0.1%			1.1%
96	2 and 11	0.1%			0.9%
97	8 and 11	0.1%			0.9%
98	31	0.1%		0.3%	
99	62	0.1%	0.03%	0.2%	0.3%
100	2 and 7	0.1%	0.1%		
101	68 and 69	0.1%	0.1%		
102	12 and 19	0.04%			0.5%

RANKING	EXON(S)	ALL MUTATIONS	DELETIONS SMALL	MUTATIONS SINGLE	EXON DUPLICATIONS
103	17 and 22	0.04%	0.1%		
104	42	0.04%		0.2%	
105	53 and 54	0.04%	0.03%		0.2%
106	57 and 58	0.04%	0.1%		
107	59	0.04%	0.03%	0.1%	
108	59 and 63	0.04%	0.1%		
109	67	0.04%			0.5%
110	73	0.04%		0.2%	
111	2 and 6	0.02%			0.2%
112	2 and 17	0.02%			0.2%
113	8 and 17	0.02%			0.2%
114	11 and 22	0.02%	0.03%		
115	17 and 20	0.02%	0.03%		
116	18 and 46	0.02%			0.2%
117	21 and 44	0.02%	0.03%		
118	22 and 43	0.02%			0.2%
119	44 and 52	0.02%			0.2%
120	46 and 52	0.02%			0.2%
121	49	0.02%		0.1%	
122	52 and 57	0.02%	0.03%		
123	58 and 62	0.02%			0.2%
124	62 and 68	0.02%	0.03%		
125	66 and 68	0.02%		0.1%	
126	71	0.02%		0.1%	
127	72	0.02%		0.1%	
128	75	0.02%	0.03%		
129	77	0.02%		0.1%	
130	78	0.02%			0.2%

Table 2. Applicability of the exon skip approach.
This table gives an overview of the proportions of patients that benefit from single or double exon skipping (From Aartsma-Rus et al. Hum. Mut 2008, reprinted with kind permission of John Wiley and Sons).

Several different AON chemistries are available to induce exon skipping, but only the 2'O-methyl phosphorothioate (2OMePS) and phosphorodiamidate morpholino oligomers (PMO) have so far been tested in clinical trials for DMD. These specific chemistries are favoured above others for their specificity and good safety profile in humans. The structure of 2OMePS AONs is similar to that of RNA, but contains two modifications. Instead of the non-bridging oxygen atom found in RNA, 2OMePS AONs contain a sulphur (atom) in the phosphate backbone, thereby forming a phosphorothioate (PS) backbone. This enhances stability by inhibiting breakdown by endo- and exonucleases. The PS backbone also facilitates low affinity binding to serum proteins, thereby preventing rapid clearance by liver and kidney upon systemic injection. This leads to a relatively long serum half-life of approximately 29 days (Goemans et al. 2011). The second modification consists of a methyl group at the 2'-OH position of the ribose sugar which renders 2OMePS AONs resistant against RNase-H mediated knockdown, and also results in higher affinity to the target RNA (Aartsma-Rus et al. 2004b).

PMOs contain six-membered morpholine rings that are connected through phosphorodiamidate linkages (Summerton and Weller 1997). They have a non-ionic backbone at physiological pH, which minimizes protein interactions and non-specific antisense effects, and increases binding capacity to mRNA. Unfortunately, their uncharged nature makes them hard to

transfect in tissue culture and results in a short half-life of ~1.6-3.6 hours upon systemic injection as they are rapidly filtered out by the kidney (Amantana and Iversen 2005;Cirak et al. 2011).

The first *in vitro* proof of concept studies were performed with 2OMePS AONs on patient-derived cell cultures carrying a variety of different mutations throughout the *DMD* gene. AON transfections resulted in the skip of the targeted exon, subsequent restoration of the reading frame and synthesis of dystrophin (Takeshima et al. 2001;van Deutekom et al. 2001;Aartsma-Rus et al. 2003). Both chemistries have also been locally administered in the *mdx* mouse where a skip of exon 23 restores the murine *Dmd* reading frame (Dunckley et al. 1998;Wilton et al. 1999). These experiments showed that also in the mouse model restoration of the reading frame resulted in dystrophin synthesis. Systemic administration revealed that dystrophic muscle is an easier AON target than healthy muscle, since 10-fold higher AON levels were detected in dystrophic compared to healthy muscles (Heemskerk et al. 2010). This is thought to results from the damaged membranes that facilitate AONs to enter the target tissue. Treated *mdx* mice had improved muscle pathology and function in the absence of toxicological side effects (Lu et al. 2003;Alter et al. 2006). PMOs were also successfully tested in some GRMD-dogs, where a double skip of exon 6 and 8 results in the correction of the reading frame and consequent dystrophin synthesis (Yokota et al. 2009).

1.1.4.2. Clinical trials

With these encouraging data, AONs targeting exon 51, which would benefit the largest group of patients, have been tested in clinical trials for both chemistries. Trials with 2OMePS AONs (PRO051/GSK2402968) were initiated by Prosensa Therapeutics, later joined by GlaxoSmithKline (GSK), while those with PMOs (AVI-4658) were undertaken by AVI-BioPharma in collaboration with the MDEX consortium. The first-in-man trial involved a single local intramuscular injection with 0.8 mg PRO051/GSK2402968 in the tibialis anterior of four DMD patients (NTR712). Biopsies taken one month later revealed that targeted exon 51 skipping resulted in 67-97% dystrophin positive fibers at levels of 17-35% of wild type (van Deutekom et al. 2007).

Later, intramuscular injections in the extensor digitorum brevis (EDL) of DMD patients with 0.09 mg (n = 2) and 0.9 mg (n = 5) AVI-4658 were performed by AVI-BioPharma and the MDEX consortium (NCT00159250) (Kinali et al. 2009). Biopsies were taken three and four weeks after administration. In all patients receiving the high dose, dystrophin restoration was found in 44-79% of the fibers at intensities ranging from 22-32% of wild type. The low dose only resulted in specific exon 51 skipping but no dystrophin synthesis. These trials showed that AON-mediated exon skipping with both chemistries was effective and safe.

The human body consists of 434 different muscles which account for 30-40% of its content. Since all these should be targeted, systemic AON delivery is crucial. Thus, after the encouraging results obtained with local administration for both chemistries and optimization of systemic treatment in animal models (Alter et al. 2006;Heemskerk et al. 2009;Heemskerk et al. 2010;Lu et al. 2005;Malerba et al. 2009), systemic trials were initiated. An open-label Phase I/II trial was undertaken for PRO051/GSK2402968 (NTR1241). Four cohorts, each consisting of three patients, received five weekly subcutaneous injections of either 0.5, 2, 4 or 6 mg/kg (Goemans et al. 2011). Biopsies revealed a dose-dependent recovery of dystrophin expression in almost all patients, of up to >80% of the fibers in patients receiving the highest dose. Maximum dystrophin signal intensity compared to wild type was 15.6% after treatment, while no adverse effects were reported. Thereupon, at the beginning of 2010, all patients enrolled in a still ongoing open label extension study (NCT01480245), receiving weekly injections of the highest (6mg/kg) dose. No serious adverse effects have been reported so far. The mild or moderate side effects so far are

reactions at the injection site, proteinuria and increased urinary α_1-microglobulin levels. After 12 weeks, this resulted in a trend of functional improvement in the 6-minute walk test in most of the patients, contrasting the anticipated decline. Results should be interpreted with caution due to the open-labelled nature of the trial and the lack of a placebo group. Therefore, to elucidate the effectiveness of the compound, as well as long term safety and tolerability, a double-blind placebo-controlled Phase III trial has been initiated involving weekly GSK2402968 administration of 6 mg/kg in 180 patients (NCT01254019). Another double-blind placebo-controlled trial, undertaken for the same compound is a Phase II trial elucidating the effects of different dosing regimens (once versus twice weekly 6 mg/kg) (NCT01153932). In addition, a Phase I trial assessing the pharmacodynamic profile of a single injection of different doses (3, 6, 9 and 12 mg/kg) in non-ambulant patients has been initiated (NCT01128855). Finally, a phase II, placebo controlled study has been initiated assessing two doses (3 and 6 mg/kg/week) in ambulant patients (NCT01462292).

AVI-BioPharma performed an open-label dose escalation Phase Ib/II trial, in which 19 DMD patients received weekly intravenous injections with 0.5, 1, 2, 4, 10 or 20 mg/kg AVI-4658 for a period of 12 weeks (NCT00844597). Exon 51 skipping was detected in biopsies from all patients, leading to a variably dose-dependent dystrophin synthesis in patients receiving 2 mg/kg or more. The maximum proportion of dystrophin positive fibers found was 55% obtained in a patient of the highest dosing cohort, while maximum fiber intensity compared to wild type levels was 27% post-treatment. As AVI-4658 also appeared to be well tolerated, a double blind placebo-controlled Phase II study has been undertaken to assess efficacy, pharmacokinetics, safety and tolerability (Cirak et al. 2011). Patients received a 60-minute intravenous infusion of 30 mg/kg (n = 4), 50 mg/kg (n = 4) or placebo (n = 4) once weekly (NTC01396239). Exon 51 skipping was detected in all patients receiving 30 mg/kg for 24 weeks, resulting in increased dystrophin levels. In biopsies from patients receiving 50 mg/kg for 12 weeks exon 51 skipping did not result in increment of dystrophin synthesis (www.avibio.com). Clinical outcome measures (6-minute walk test, Gower's maneuver, 10 meter run) did not change in any of the treatment groups. As no serious side-effects were reported, all patients enrolled in an open-label extension study. Patients belonging to the placebo group are now also receiving AVI-4658.

Although no apparent differences in efficiencies regarding both proportion of dystrophin positive fibers and their expression levels were observed between the two chemistries upon intramuscular injection, these were observed upon systemic administration. Compared to the PRO051/GSK2402968 trial where doses dependent dystrophin expression (in up to 80% of the fibers) was observed in roughly all (10 out of 12) patients, the AVI-4658 trial reported to observe restored dystrophin expression in 55% of the fibers or less in only a few (7 out of 19) patients. This might be due to technical differences in immuno-histochemical protocols, reference samples and analysis methods used in the two studies. On the other hand, biological factors might underlie this difference. As previously mentioned, the serum half-life of 2OMePS (<4 to 28 days) and PMOs (1.6 to 3.6 hours) differs significantly. Since PMOs are quickly cleared by the liver and kidney, the chances of being taken up by muscle are lower for PMO than for 2OMePS AONs. Possibly, and consistent with the greater variability observed for PMO, the much lower effective muscle exposure with PMO leads to variable uptake of AONs dependent on the physical integrity of specific fibers, with recently disrupted/repaired fibers taking up more AON. Further studies are needed to elucidate the exact cause for the differences in dystrophin expression found upon systemic administration.

Effort is also put in the development of AONs targeting other exons. Currently, Prosensa Therapeutics conducts a dose escalation trial with 2OMePS AON targeting exon 44 (PRO044) which would apply to 6% of patients (NCT01037309). This open-label Phase I/IIa trial consists of weekly subcutaneous injections of 0.5, 1.5, 5, 8, 10 and 12 mg/kg PRO044 for 5 weeks. Pre-clinical investigations for AONs targeting exon 45, 53, 52 and 55 are ongoing and it is anticipated that exon Phase I/IIa trials for exon 45 and 53 will be initiated in 2012.

1.1.4.3. Hurdles to overcome

Even though AON-mediated exon skipping results in restoration of dystrophin expression and is well tolerated, there are still several hurdles to overcome. As previously mentioned, skeletal muscle fibers of DMD patients have an uptake advantage as AONs can easily enter the fibers through disruptions of the membrane. However, mouse studies indicate that large amounts are still taken up by liver and kidney. To improve delivery to muscle, AONs may be bound to sugar groups or cell-penetrating peptides. The efficiency of the latter has been investigated to enhance uptake of PMOs in mouse models. Cell-penetrating, arginine-rich peptides were conjugated to PMOs (PPMO) and injected in *mdx* and *mdx/utrn* $^{-/-}$ mice. This resulted in increased intracellular PPMO levels and very efficient dystrophin restoration, leading to improved functional performance and life span in the severely affected *mdx/utrn* $^{-/-}$ mouse. No adverse effects were observed in both models (Goyenvalle et al. 2010;Yin et al. 2008;Moulton et al. 2009). Based on these encouraging results, PPMOs targeting exon 50 (AVI-5038) were further tested in primates in preparation for a clinical trial. Unfortunately, the toxicity observed after systemic administration has precluded further development of this specific compound (Sazani et al. 2009). As differences in chemistry might resolve the toxicity issue, pre-clinical investigations aim at identification of non-toxic peptides that enable targeted AON uptake (Yin et al. 2009;Yin et al. 2010;Yin et al. 2011).

Additionally, also the heart is more challenging to target (Heemskerk et al. 2010). This is probably due to differences in architecture of cardiomyocytes, which are not as permeable as skeletal muscle fibers and thus have a more limited AON uptake. The consequences of AON-induced dystrophin expression in skeletal muscle in the absence of expression in heart are unknown. It is speculated that as dystrophin expression in skeletal muscle will result in increased activity levels, a higher workload will be projected to the heart, which might worsen heart disease progression (Malerba et al. 2011a;Townsend et al. 2008). Other reports indicate that dystrophin correction of diaphragm itself is already beneficial for heart function in dystrophic animal models (Crisp et al. 2011). As more than 90% of DMD patients develop dilated cardiomyopathy, applying some form of cardiac therapy is essential. In principle, heart transplantation is an option but this may not always be a viable approach dependent on organ availability, condition and histocompatibility status. Thus preferably also the heart would need to be targeted.

As yet, it remains unknown which levels of dystrophin are needed to protect muscles against damage and prevent or delay disease progression. From case reports, and studies in BMD and DMD patients and BMD carriers it has been speculated that ~20% already results in a mild phenotype (Hoffman et al. 1988;Hoffman et al. 1989;Neri et al. 2007). With new mouse models expressing variable, low dystrophin levels more insight in this issue has been gained (Chapters 4, 5 and 6).

As AON-mediated exon skipping is a personalized approach leading to the production of dystrophins that internally lack different sequences, it can only be speculated whether these proteins differ in performance. It might be that deletion of specific parts differentially affects the

ability to protect against fiber damage, protein stability or secondary pathology (eg. brain involvement). Additional factors might also play a role as differences in severity within BMD families have been reported (Melis et al. 1998). Upcoming clinical trials will probably give more insight in these issues.

Finally, DMD is a rare disease affecting only 1:3500 newborn boys and mutations are present throughout the entire gene. To treat all patients that might theoretically benefit from this approach 130 combinations of single and double exon skipping are needed targeting more than 50 different exons (Aartsma-Rus et al. 2009) (Table 2).

1.2. Mouse models for DMD

1.2.1. The *mdx* mouse

The most commonly used mouse strain in DMD research is the *mdx* mouse. This is a natural model which arose from the C57BL/10ScSnJ (wild type) strain. It was first described in 1984 under the official name C57BL/10ScSn-*Dmd*^{mdx}/J (Bulfield et al. 1984), where *mdx* stands for: X-linked muscular dystrophy. *Mdx* mice have a point mutation in exon 23 of the *Dmd* gene (A>T at base 3185 replacing a glutamine codon (CAA) with a termination codon (TAA)). This premature stop codon prevents synthesis of full-length dystrophin (Sicinski et al. 1989). Even though only 15% of the DMD patients have a nonsense mutation, this model has been of great importance for proof of concept studies of potential therapeutic approaches like exon skipping and compounds targeting premature stop codons.

Although both DMD patients and *mdx* mice lack full-length dystrophin, the pathology of *mdx* mice is less severe (see below), enabling them to almost live as long as wild type mice and making homozygous breeding possible. The mean age of wild type mice is 27 and 26.5 months for females and males respectively, whereas this is 22.5 and 21.5 months for female and male *mdx* mice respectively (a reduction of 17% for females and 19% for males) (Chamberlain et al. 2007). In addition, slightly higher (~3.5 fold) mortality levels have been observed in *mdx* pups. Also the number of young *mdx* mice that die before the age of seven days is 45% higher than wild type mice (Torres and Duchen 1987). These rates seem to be independent of litter size, but as *mdx* mice are very susceptible to stress, mortality can be reduced by reducing animal handling and regular cage cleaning.

1.2.1.1. Skeletal muscle histopathology

The initiation of muscle pathology in *mdx* mice is essentially identical to that in DMD patients. However, in *mdx* mice, pathogenesis occurs in waves and is not a continuum like in DMD patients. Until weaning, only minor pathological changes have been reported (Grounds et al. 2008). From the age of 3-4 weeks onwards, an acute onset of degeneration followed by regeneration is present, which lasts for five weeks and then subsides (Bulfield et al. 1984). The cause for the acute onset instead of a more gradual one is unknown. As a result, loss of muscle fibers is slow in adult *mdx* mice, with regenerated fibers being more resistant to necrosis. More severe muscle weakness is only found in old *mdx* mice with the diaphragm being the most severely affected muscle. Replacement of fibers by fat tissue is rare (Chamberlain et al. 2007;Stedman et al. 1991;Bulfield et al. 1984;Deconinck et al. 1998;Karpati et al. 1988;Weller et al. 1990).

For obvious reasons, pathological events in mice can be studied in more detail than in DMD patients, where generally only biopsies are available (Figure 8). Histopathology is characterized by increased numbers of small, newly regenerated fibers, as well as big hypertrophic fibers and by large patches of fibrosis and necrosis (Marshall et al. 1989). Like DMD patients, *mdx* mice also have revertant fibers and these increase in number with age from ~11 fibers in one month old to >100 in one year old mice. *Mdx* mice that are irradiated with 18 Gy have significantly reduced muscle regeneration and consequently a reduced expansion of their revertant fibers. Revertant fibers in heart do not increase in number over time (Yokota et al. 2006;Lu et al. 2000).

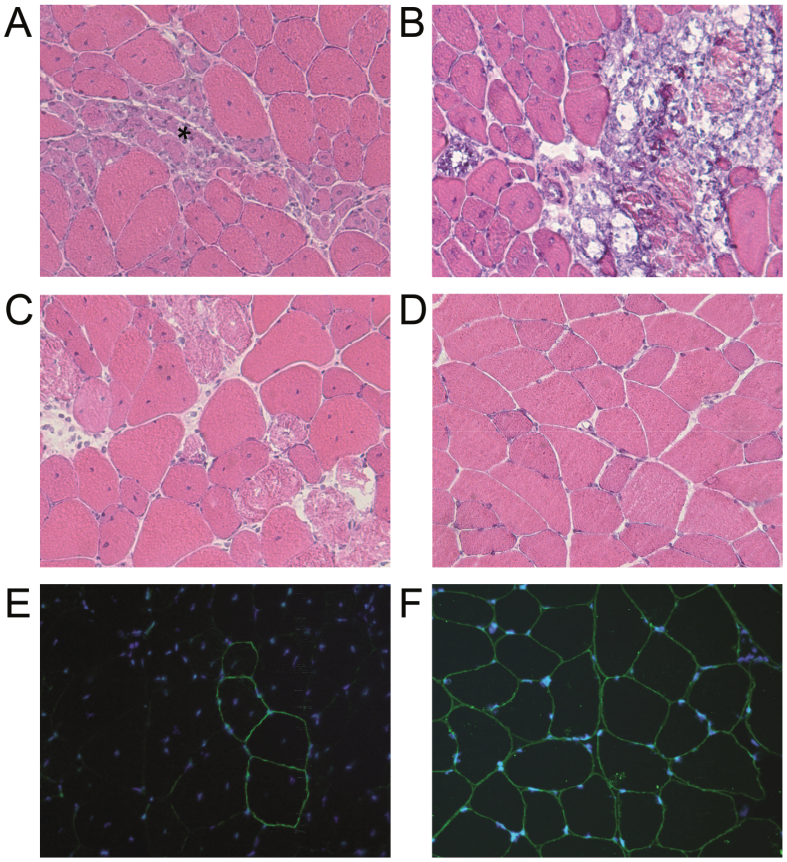

Figure 8. Cross sections of the quadriceps of an *mdx* and a C57BL/10ScSnJ (wild type) mouse.
A. The *mdx* mouse section shows a lot of variation in fiber size, with small, newly regenerated fibers and enlarged hypertrophic fibers. Most fibers have centralized nuclei, indicating recent regeneration events. Newly regenerated fibers are indicated with an arrow. **B**. Pathology in an *mdx* mouse involving an area with fibrosis and infiltration of inflammatory cells. **C**. Fibers undergoing necrosis in a section of an *mdx* mouse. **D**. C57BL/10ScSnJ mouse reveals muscle fibers that are evenly sized and with nuclei at the membrane. No pathological features are evident. **E**. Revertant fiber in an *mdx* cross section. **F**. Dystrophin expression of a C57BL/10ScSnJ mouse.

Muscle fibers of *mdx* mice also have an abnormal architecture as they can have one or multiple branches (Head et al. 1992;Lovering et al. 2009). Different types of branches have been found; fibers being totally split in two (Y-shape), having one or multiple small branches on the side (╣ shape), or having a small split in the middle while remaining intact at either side. It is hypothesized that branches originate from imperfect fusion of myogenic cells during regeneration. Branched fibers are more susceptible to exercise-induced damage. The number and complexity of the branches increases with age as in young *mdx* mice (6-8 weeks old) 17% of the fibers have branches, while this increases to 89% in old (27-31 weeks old) mice. Only in old *mdx* mice these branches result in a significantly increased drop in maximum tetanic force upon repeated eccentric contractions of 58% in *mdx* compared to 25% in wild type mice. Fibers of wild type mice rarely have branches (Chan et al. 2007;Chan and Head 2011).

1.2.1.2. Neuromuscular junction and skeletal muscle pathology

Mdx mice have abnormalities in the anatomy of the NMJ and show functional deficits in muscle. To better appreciate the significance of these abnormalities and those observed in other DMD mouse models, the situation in wild type mice is discussed first, followed by that in *mdx* mice.

Muscle contractions are coordinated by the central nervous system, from which nerve pulses are sent to the NMJ (Figure 9). When these reach the synaptic end bulb, acetylcholine (ACh) is released from vesicles and diffuses across the synaptic cleft to bind ACh receptors (AChR) at the motor end plate of the muscle. This causes ion channels to open which allow entrance of Na^+ into the muscle fiber resulting in an action potential. The action potential travels across the sarcolemma and initiates the muscle to contract (see below). ACh is then broken down by acetylcholinesterase (AChE) in choline and acetate in the synaptic cleft. Dystrophin and utrophin colocalize with the Na^+ channels at the base of the folds and with the AChRs respectively. Although utrophin compensates for the lack of dystrophin in the muscular sarcolemma, compensation for each others absence does not happen in the NMJ. The DGC is involved in the maturation and cluster formation of AChRs, in the regulation of ACh release and maintenance during NMJ differentiation (Deconinck et al. 1997a;Grady et al. 1997a;Miike et al. 1989;Pilgram et al. 2010;Grady et al. 2000).

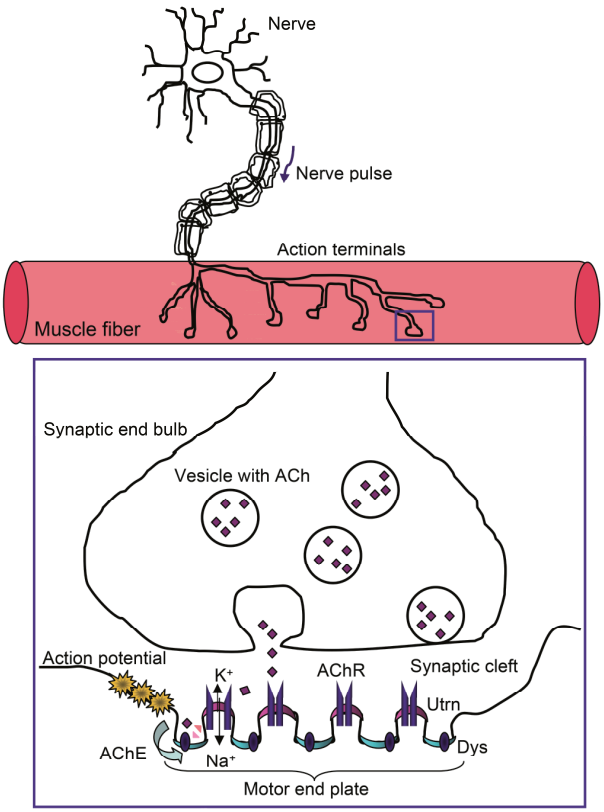

Figure 9. The neuromuscular junction.
Nerve pulses excited by the central nervous system ensure release of ACh in the synaptic cleft. Uptake of ACh by AChR results in an influx of Na^+ in the motor end plate of the muscle provoking an action potential which eventually ensures muscle contraction. (Figure adapted from http://www.educarer.com).

In comparison to wild type mice, the NMJ motor end plate of *mdx* mice displays varying decrease of postsynaptic folding, whith ~30% of the area completely lacking folding. Additionally, AChRs and AChEs are abnormally distributed from the age of 4-6 weeks onwards. α-Bungarotoxin staining (visualizing AChRs) reveals that synapses of *mdx* mice consist of distinct boutons whereas continuous branches are present in wild type mice (Lyons and Slater 1991;Ferretti et al. 2011). Electrophysiological properties of the NMJ are not impaired as the total number of AChRs and AChEs remains similar. Interestingly, all these pathological hallmarks are only observed in regenerated fibers, indicating that the lack of dystrophin itself has minor direct consequences. However, during regeneration in the absence of dystrophin, utrophin clustering is altered which results in remodelling of the pre- and postsynaptic components (Lyons and Slater 1991;Ferretti et al. 2011).

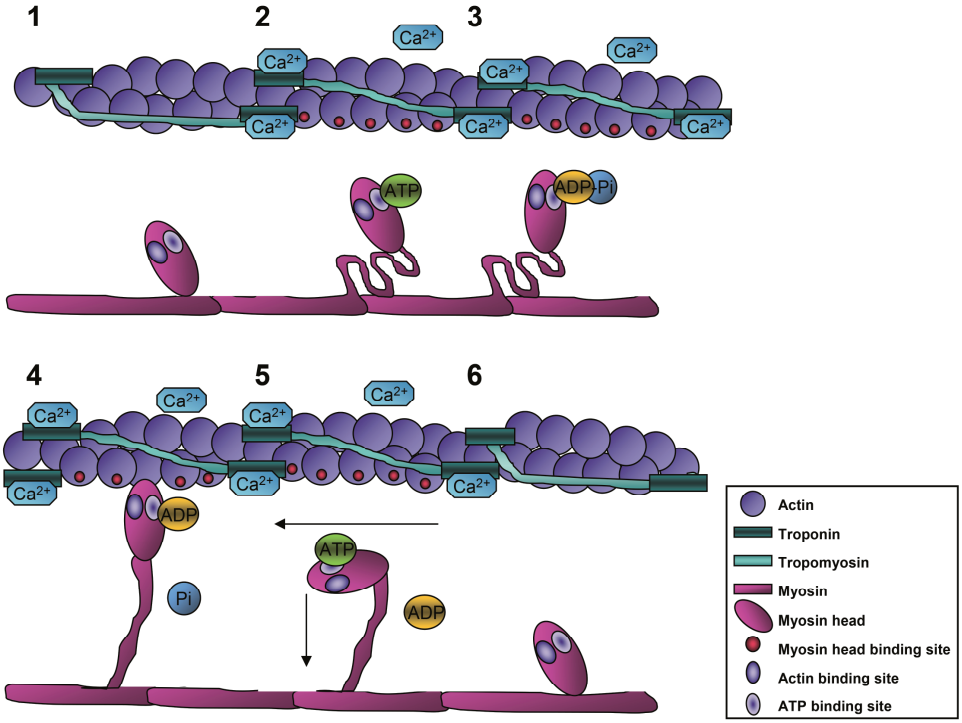

Figure 10. Molecular mechanisms of a muscle contraction.
1. Upon arrival of the action potential in the T-tubules, Ca^{2+} is released from the sarcoplasmic reticulum and binds to Troponin C in the myofibril. **2.** This ensures a conformational change of tropomyosin exposing the myosin head binding sites. **3-5.** Cycles of ATP triggered binding and release of the myosin head to actin, bring them in close proximity of each other resulting in contraction of the muscle. **6.** Upon depletion of Ca^{2+}, the conformational change of actin will be reversed, making myosin head binding sites inaccessible. Thereupon, actin slides back in its original position resulting in muscle relaxation.

The action potential from the NMJ is transported over the sarcolemma and ends up in the T-tubules located in the core of the muscle fibers. This triggers opening of voltage sensitive proteins and thereby release of Ca^{2+} from the sarcoplasmic reticulum in the cytosol. Within the myofibril, Ca^{2+} binds to Troponin C in the actin filaments of the sarcomere, changing the conformation of tropomyosin ensuring exposure of myosin head binding sites (Figure 10 step 1). Contractions start with the binding of ATP to the myosin head (step 2), which contains the

enzyme adenosine triphosphatase (ATPase) which splits ATP into ADP, phosphate and energy (step 3). This triggers the myosin head to bind to the actin filament. This initial binding is tightened by release of the phosphate molecule (step 4). Conformation of proteins in the myosin head lead to their repositioning and thereby pulls the actin filament along the myosin. Upon binding of another ATP molecule to the myosin head it moves back to starting position and the ATP is broken down into ADP and phosphate (step 5). Binding of a new ATP molecule will repeat this procedure, but leads to a more proximal binding so that the myosin and actin filaments are brought towards each other resulting in muscle contraction. In the absence of new Ca^{2+}, tropomyosin will move back in its original conformation. This depletes the number of myosin head binding sites, forcing actin to slide back in its previous location leading to muscle relaxation (step 6) (Holmes 1996).

The myotendinous junction (MTJ) is located at the distal sides of a muscle where it is connected to the tendon. In wild type mice, the MTJs are extensive finger-like projections of the sarcolemmal membrane, which serve to increase the area of attachment between the muscle fiber and the tendon. They also ensure force transmission between muscle and tendon. Like the NMJ, also in the MTJ a marked reduction in the number of foldings is observed in *mdx* mice (Law and Tidball 1993;Deconinck et al. 1997b).

There are three main types of muscle contractions; isotonic (muscle shortens as force generated is greater than the load), isometric (load is greater than force generated, muscle length remains similar) and isokinetic (same speed) contractions. Isotonic contractions can be divided into two groups; concentric and eccentric contractions. During concentric contractions muscle contract and shorten in length, eccentric contractions result in lengthening of the muscle. In the latter case, muscles not only contract to build force but also slide alongside each other to lengthen. Muscle contractions in *mdx* mice have been studied in individual fibers and whole muscles. The most often used outcome measures are twitch force (force generated upon a single stimulation), tetanic force (force generated upon summation of individual twitches) and muscle fatigue initiated by multiple eccentric contractions.

Acute weakness of the proximal followed by the distal muscles is observed in young *mdx* mice during the cycles of degeneration and regeneration (Muntoni et al. 1993). Although hypertrophic fibers generate higher twitch force than wild type mice, the relative force normalized for cross sectional area is significantly decreased in both young and old *mdx* mice. Force generating capacity of 21 months old *mdx* mice differs between fast and slow muscles. Fast muscles have significantly decreased twitch and tetanic force as well as decreased resistance to eccentric contractions, whereas slow muscles only have a significant decreased tetanic force compared to wild type muscle (Bobet et al. 1998;Lynch et al. 2001;Raymackers et al. 2003). Muscle force also differs between male and female mice as in females tetanic force is significantly less impaired at the age of six months (Hakim and Duan 2012). Impaired muscle function of *mdx* mice results in significantly reduced voluntary activities and bad overall motor performance (section 1.4.1.5.) (Hara et al. 2002;van Putten et al. 2012). However, chronic voluntary wheel running activities improve tetanic force of the EDL by 28% (Call et al. 2010). On the other hand, muscle pathology can also be negatively influenced by chronic horizontal treadmill running, which puts increased strain on the muscles. Especially downhill running in which muscles are mainly challenged by eccentric contractions result in very severe pathology (Wooddell et al. 2010).

1.2.1.3. Pathology of the heart

Like DMD patients, *mdx* mice also develop dilated cardiomyopathy resulting from an identical pathological cascade. Heart function has been primarily studied by ECG and MRI (section 1.4.2.). In mice, the first pathological hallmarks are observed from the age of 2-3 months onwards. These involve uptake of Evans blue dye by cardiomyocytes, lower levels of nNOS and increased strain and tension (van Erp et al. 2010;Bia et al. 1999). In a proportion of *mdx* mice abnormal S-waves are observed. Mice aged 6 months have significantly higher levels of fibrosis and macrophage infiltrations than wild type mice, and these increase in proportion with age. Fibrosis is not restricted to a particular region, but is distributed in a patchy manner over both ventricles (Li et al. 2009). In parallel, elevated levels of markers involved in ECM remodeling and fibrosis (amongst others; CTGF, TIMP-1, MMP-9 and TGF-β1) are found as well (Au et al. 2011). Additionally, hypertrophy of the heart involving in particular the left ventricle has been described. ECGs of these mice are characterized by polyphasic R-waves and decreased S/R ratios. More extensive impairment of heart function is present from the age of 7-8 months onwards. First a decrease in right ventricular ejection fraction is observed accompanied by a decreased end diastolic volume and increased end systolic volume. In slightly older mice, a decreased left ventricular ejection fraction is observed as well (Figure 11). Some articles have reported a decreased cardiac output of both ventricles in 9-10 months old mice. A decreased S and R wave amplitude and increased heart rate is present at the age of 12 months.

Discrepancy exists in literature regarding the age of onset of dilated cardiomyopathy, as some studies report these changes at an early age (Verhaart et al. 2011;Zhang et al. 2008;Crisp et al. 2011) while others do not observe major functional abnormalities in 10 months old *mdx* mice (Li et al. 2009).

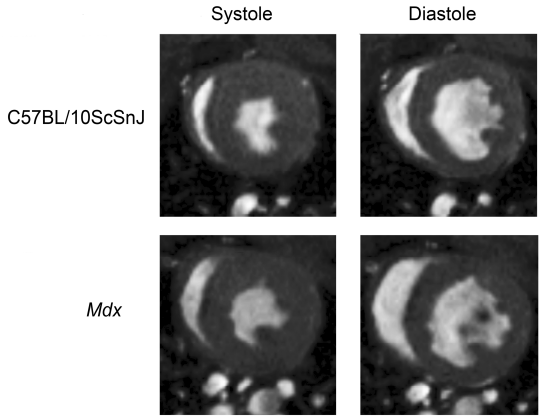

Figure 11. MRI scans of the heart of a C57BL/10ScSnJ and *mdx* mouse.
MRI scans of the systolic and diastolic phase of the heart contraction from a wild type and *mdx* mouse aged 10 months. At this age, *mdx* mice show severe dilatation of both the left and right ventricles, involving decreased stroke volume and ejection fraction.

The exact cause for this is unknown, but it might be due to differences in the wild type strains used (C57BL/10ScSnJ versus C57BL/6). Also gender is known to influence heart function as this is more severely impaired in 22 months old female compared to male *mdx* mice (Bostick et al. 2010).Forced treadmill exercise or voluntary wheel running has been found to negatively influence heart function most likely by putting an increased workload and strain on the heart (Costas et al. 2010;Nakamura et al. 2002).

1.2.1.4. Limitations of the mdx mouse

Although *mdx* mice and DMD patients share the genetic defect that hampers the expression of functional dystrophin, pathology is less severe in mice. In contrast to DMD patients, motor function of *mdx* mice is only slightly reduced, they do not lose the ability to walk and life span is only slightly shorter. These differences can primarily be explained by differences in body size and architecture. The time-scale in which mice grow and mature is much shorter than that of humans, as mice directly go from childhood into adulthood, while humans spend a significant period of their life in puberty. This means that only 5% of a mouse's total life span has passed before they become sexually mature, while this is 20% for humans. Developmental milestones of DMD patients have been compared with *mdx* mice based on hormonal and physiological changes (Table 3) (Grounds et al. 2008). This clearly showed that the time-frame in which *mdx* mice undergo major pathological changes is extremely short in comparison to DMD patients. Mice also have a much smaller body size and distribute their body weight over four limbs instead of two. Taken together, this reduces the workload and stress on the muscles, preventing damage.

Human	Mouse
Newborn	1 week
~3 months	2 weeks
~6 months	3 weeks
~10 months	4 weeks
~16-18 years	6 weeks
~20 years	8 weeks
~25 years	12 weeks

Table 3: Developmental comparison between human and *mdx* mouse.
Based on hormonal and physiological changes, Grounds et al. published this comparison between DMD patients and the *mdx* mouse. It can be appreciated from the table that most of the DMD pathology falls within the first eight weeks of the mouse's live (From Grounds et al. Neurobiol. Dis. 2008; reprinted with permission of Elsevier)

The less severe pathology observed in *mdx* mice results from multiple additional factors. *Mdx* mice have an incredible regeneration capacity for exceeding that of DMD patients. Furthermore, expression of transcription factors like Myod is upregulated, which enhances regeneration. Muscles of *mdx* mice are also better protected against damage since they are more efficient in overexpressing the dystrophin homologue utrophin that can functionally compensate for the loss of dystrophin. Also in DMD patients, utrophin is overexpressed between 2 and 10-fold compared to healthy controls, and these levels do positively correlate with disease severity (Kleopa et al. 2006). However, compensation in mice is more effective than that in human. This might be caused by differences in fiber diameter between human and mouse. As the surface-to-volume ratio is smaller in human, the sarcolemma of these fibers experiences more stress and therefore they might require more utrophin (Grady et al. 1997b). It is not known whether the compensatory mechanisms of mice will generate similar protective effects in human, as overall size and forces placed on muscles are different.

1.2.2. The *mdx*$^{2\text{-}5cv}$ mouse models

In addition to the naturally occurring *mdx* mouse, several other mice with mutations in the *Dmd* gene have been generated to make more extensive studies possible (Chapman et al. 1989). Male C3H.X$_{25}$ x C57BL/6Ros mice were intraperitoneally treated with the chemical *N*-ethylnitrosourea (ENU). This chemical is a powerful mutagen inducing point mutations to progeny at a frequency of 1 mutation per 700 loci. Crossings of ENU treated males with C57BL/10 x *mdx* females resulted in female progeny which were selected according to their CK level. This resulted in four *mdx* models with mutations throughout the *Dmd* gene, called *mdx*^{2cv}, *mdx*^{3cv}, *mdx*^{4cv} and *mdx*^{5cv}. Mutations of these mice, consisting of one nonsense and three affecting mRNA splicing were found to be spread over the gene, making these mice an ideal object to study the effect of mutation position on pathology (Cox et al. 1993;Im et al. 1996).

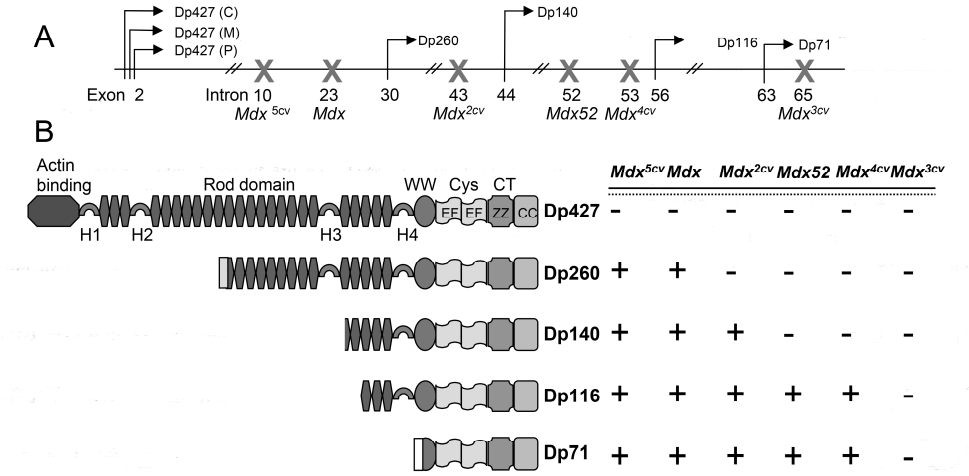

Figure 12. Dystrophin isoforms in different *mdx* mouse models.
A. Representation of the *Dmd* gene in which the induced or natural mutations of the *mdx*^{cv}, *mdx52* and *mdx* mouse models are indicated by a cross. **B**. This schematic overview summarizes which isoforms are expressed in the *mdx*^{cv}, *mdx52* and *mdx* models. (Figure is based on Willmann et al. NMD 2009).

The *mdx*^{2cv} mouse has a single base mutation (A>T) in the acceptor splice site of exon 43 (which lies in intron 42) of the *Dmd* gene. This mutation results in a complex pattern of aberrant splicing that generates multiple transcripts, of which none has an intact reading frame, so that the synthesis of functional full-length dystrophin synthesis is prevented. The smaller isoforms Dp140, Dp116 and Dp71 are normally expressed in these mice (Figure 12). The *mdx*^{3cv} mouse carries a T>A mutation in intron 65 (14 base pairs proximal to exon 66), which introduces a cryptic splice site and frame-shift that prevents completion of all dystrophin isoforms. This makes *mdx*^{3cv} mice exceptional since all other known *mdx* substrains express Dp71 and one or multiple additional short dystrophin isoforms. *Mdx*^{4cv} mice have a C>T transition (CAA to TAA) at position 7916 in exon 53, which results in a premature stop codon, preventing dystrophin synthesis. These mice express only the dystrophin isoforms Dp116 and Dp71 (Im et al. 1996). *Mdx*^{5cv} mice have an A>T mutation at position 1324 of exon 10. This mutation introduces a cryptic splice donor site (GTGAG) that generates a frame shift and prevents the synthesis of dystrophin (Im et al. 1996). As this mutation is close to the N-terminus of the protein, these mice only lack full-length dystrophin and express all the short dystrophin isoforms, like *mdx* mice.

Initially, it was thought that pathology of the *mdx*$^{2\text{-}5cv}$ mice greatly corresponded with that of *mdx* mice, therefore only mice younger than six months were studied. However, detailed investigations carried out in non-muscle tissues revealed phenotypical differences resulting from the absence of specific dystrophin isoforms. As the *mdx*^{3cv} mouse does not express any dystrophin isoform, this model has been most intensively studied. *Mdx*^{3cv} mice appeared hard to breed and survival chances of pups were smaller than that of *mdx* mice. Also the litter size is much smaller, which is not the case for the other *mdx*^{cv} models (Cox et al. 1993). Mouse spermatozoa contain Dp71. Spermatozoa lacking Dp71 have abnormally shaped flagella and altered distribution of ion channels and signalling proteins. Although the short utrophin isoform Up71 is upregulated and redistributed and levels of α-syntrophin and voltage dependent Na^+ and K^+ channels are increased in *mdx*^{3cv} mice, this does not prevent the phenotype (Hernandez-Gonzalez et al. 2005).

Besides differences in fertility, *mdx*^{3cv} mice also differ on a histological level from the other *mdx*^{cv} mice. Danko et al. compared the number of revertant fibers between the *mdx*^{cv} and *mdx* mice (Danko et al. 1992). He observed that *mdx*^{3cv} mice do not express revertant fibers while *mdx* mice and the other three *mdx*^{cv} strains do. In contrast, *mdx*^{3cv} express a nearly full-length dystrophin (415kDa) at very low levels (~5% of normal levels) in all skeletal muscle fibers, but not in heart. These dystrophin proteins result from alternative splicing of the transcript, and lack the cysteine-rich domain sequences encoded by exon 65 and 66. Among the other *mdx*^{cv} mice differences in the number of revertant fibers and the amount of increment of fiber numbers over time are found. *Mdx*^{2cv} mice express 10 times more revertant fibers in skeletal muscle at the age of two and six months in comparison to *mdx*^{4cv} and *mdx*^{5cv} mice. With age, the number of revertant fibers increases 7.4 times, while increases of 4 and 4.6 times are found in *mdx*^{4cv} and *mdx*^{5cv} mice respectively. In this perspective, *mdx*^{2cv} mice are most comparable to *mdx* mice. Also in heart, the highest numbers and biggest clusters of revertant fibers are found in *mdx*^{2cv} mice. *Mdx*^{3cv} mice express revertant fibers in heart at the age of six but not two months.

Muscle function of the majority of the *mdx*^{cv} models is indistinguishable from *mdx* mice. The *mdx*^{5cv} mouse is an exception as a recent publication showed that they have functional deficits exceeding those observed in *mdx* mice. *Mdx*^{5cv} mice perform significantly worse on the rotarod and have more severe strength deficits in the diaphragm. No differences in force generation have been observed for the EDL and histopathology is also comparable between the two strains (Beastrom et al. 2011). Differences in genetic background probably underlie these findings, as differences in e.g. functional tests have been described before between different wild type strains (Connolly et al. 2001).

More distinct phenotypes have been observed in non-muscle tissues. The dystrophin isoforms Dp427, Dp260, Dp140 and Dp71 are expressed in the retina of both mouse and human. The function of the retina can be measured with an electroretinogram (ERG) which measures the electrophysiological response of the retina to light stimulation. DMD and BMD patients have abnormal ERG waveforms characterized by a reduced scoptopic b-wave. Severity of ERG abnormality is mutation specific; patients with mutations 3' have abnormal ERGs while these are normal in most patients with 5' mutations (Pillers et al. 1999;Pillers et al. 1995). To elucidate the correlation between position of the mutation and ERG severity, *mdx*^{cv} mice have been intensively studied. *Mdx*^{5cv} and *mdx* mice lacking only Dp427 have ERG waves comparable to those of wild type mice. All other strains that lack the retina isoform Dp260 have a phenotype, which differs in severity between them. *Mdx*^{2cv} and *mdx*^{4cv} mice show increased b-wave and oscillatory potential implicit times. *Mdx*^{3cv} mice are most severely affected and show in addition to increased b-wave and oscillatory potential implicit times also reduced b-wave amplitudes (Pillers et al. 1995). The mutation specific phenotype is caused by the different sites of expression, where Dp427, Dp260

and Dp140 are expressed at the outer plexiform layer of the retina, while Dp71 is expressed at retinal blood vessels and the inner limiting membrane (Howard et al. 1998). In addition, cones also have a higher Dp427 to Dp260 ratio than rods (Wersinger et al. 2011). As colour blindness is caused by non-functional rods, this nicely correlates to the finding that DMD patients who lack Dp260 more often present a deficit in red-green discrimination (Costa et al. 2007).

Also in brain, several dystrophin isoforms are expressed. Primarily *mdx*^{3cv} mice have been used to study the consequences of additional loss of all the other dystrophin isoforms. It was hypothesized that especially the loss of Dp140 and Dp71 might result in subtle abnormalities during brain development because these proteins are highly expressed in foetal brains (Lidov 1996). Studies investigating spatial learning abilities showed no differences in acquisition rates between *mdx*^{3cv}, *mdx* and wild type mice (Vaillend et al. 1995;Vaillend et al. 1998). Like in *mdx* mice, the retrieval of long term memory and synaptic transmission is unaltered in *mdx*^{3cv} mice, however differences in strategies to learn the task have been observed between these mice. In contrast to *mdx* mice, anxiety-related behaviour of *mdx*^{3cv} mice is enhanced, whereas locomotion is reduced compared to wild type mice (Vaillend and Ungerer 1999). Strangely, the ability of *mdx*^{3cv} mice to learn to press a bar is in the acquisition phase almost comparable to that of wild type, while *mdx* mice perform much worse. Performance in the extinction phase however is similar between all mice. The differences observed between *mdx* and *mdx*^{3cv} mice might be caused by the expression of low dystrophin levels in *mdx*^{3cv} mice and/or the different genetic backgrounds. However, more extensive research is needed to elucidate the exact mechanisms.

1.2.3. The *mdx52* mouse

As only a limited number of DMD patients carry point mutations, the *mdx52* mouse was generated to mimic a frequently found deletion in humans (Araki et al. 1997). In this mouse exon 52 of the *Dmd* gene was disrupted by means of homologous recombination on a C57BL/6J background. These mice lack, similar to *mdx*^{4cv} mice, full-length dystrophin and the shorter isoforms Dp260 and Dp140. Pathology and muscle function is similar to that of *mdx* mice. Hypertrophy of limb muscles is present in four months old mice along with variation in fiber size and central nucleation in 90% of the fibers. At this age also the diaphragm is more severely affected than the tibialis anterior and EDL. Revertant fibers are occasionally observed. There are no pathological changes in the heart and brain nor have behavioural changes been identified in 18 months old mice.

These mice have also been used to explore the applicability of exon 51 skipping. PMOs targeting exon 51 induced exon skipping resulted in synthesis of truncated but functional dystrophin in the absence of adverse effects (Aoki et al. 2010).

1.2.4. The *mdx/utrn* $^{-/-}$ mouse

Disease pathology of *mdx*, *mdx*^{cv} and *mdx52* mice is relatively mild in contrast to that of DMD patients, which is partly caused by functional compensation for dystrophin through the upregulation of utrophin. It was hypothesized that absence of both proteins would result in a more severe model, which would accelerate research. Therefore, effort was put into making a utrophin knockout mouse (*utrn* $^{-/-}$) to be used to generate a dystrophin and utrophin knockout mouse. However, as spontaneous mutations in the utrophin gene had never been found, it was believed that mice lacking this protein would not be viable (Grady et al. 1997a;Pearce et al. 1993). Despite these speculations, two independent groups successfully generated *utrn* $^{-/-}$ mice (Deconinck et al. 1997a;Grady et al. 1997a).

In 1997, Deconinck et al. made a construct in which an NH2 terminal exon of the *Utrn* gene, which is located in the actin-binding domain, was missing. They transfected embryonic stem (ES) cells with this construct and generated *utrn* $^{+/-}$ mice which were crossed to obtain *utrn* $^{-/-}$ mice. The mutation led to the complete loss of full-length utrophin (Deconinck et al. 1997a). Simultaneously, Grady et al. generated *utrn* $^{-/-}$ mice in which the COOH-terminal cysteine-rich region of the *Utrn* gene was removed, which is needed for binding to the DGC (Grady et al. 1997a). To do so, ES cells with this mutation generated by homologous recombination were implanted and resulted in germ line chimeras. *Utrn* $^{-/-}$ mice were again produced from crossings of *utrn* $^{+/-}$ mice. Despite the slight difference in the way utrophin expression was abolished, both models were phenotypically normal. Therefore, phenotypes of both mice will be discussed together, without making any distinctions.

Despite expectations, *utrn* $^{-/-}$ mice appeared to be viable and able to produce normal litter sizes. They did not develop any dystrophic phenotype or behavioural abnormalities and even two year old mice were indistinguishable from age-matched wild type mice in prospect of muscle function. As utrophin normally clusters with AChRs of the NMJ, a subtle phenotype was expected. Although synapses of *utrn* $^{-/-}$ mice had a normal architecture, AChRs density was 30% lower than that of *utrn* $^{+/-}$ mice, postsynaptic currents were altered and the number of postsynaptic folds of the NMJ was lower in *utrn* $^{-/-}$ mice than these of *mdx* and *utrn* $^{+/-}$ or $^{+/+}$ mice. Although utrophin was missing from the synaptic sites, the synaptic DGC complex was maintained and no decrease in levels of any of the proteins was observed, probably as a consequence of dystrophin somehow making up for the utrophin absence. As discussed in section 1.1.2.1, the distribution of utrophin and dystrophin does not overlap in the NMJ. It was assumed that the DGC complex would be unaffected in the *utrn* $^{-/-}$ mice as a result of replacement of utrophin by dystrophin. Investigations however revealed that this was not the case as dystrophin was evenly distributed with no synaptic enrichment. Dystrophin did also compensate for utrophin in several other organs like brain, kidney and heart (Deconinck et al. 1997a;Grady et al. 1997a).

As *utrn* $^{-/-}$ mice were viable and free from any dystrophic phenotype, both research groups crossed them with *mdx* mice to obtain mice lacking both dystrophin and utrophin. These mice were called *mdx/utrn* $^{-/-}$ or double knockout (dko) mice (Deconinck et al. 1997b;Grady et al. 1997b). Extensive studies have been carried out, elucidating the consequences of the lack of both proteins in mice. In accordance with the two *utrn* $^{-/-}$ mouse models, no phenotypical differences have been described for the two *mdx/utrn* $^{-/-}$ strains. Therefore no distinction will be made between the two from now on.

Mdx/utrn $^{-/-}$ mice are much more severely affected than *mdx* mice and closely mimic the phenotype of DMD patients. At birth, *mdx/utrn* $^{-/-}$ pups have a similar appearance as *mdx* and

wild type pups. However, from weaning onwards, *mdx/utrn* $^{-/-}$ mice are significantly smaller than *mdx* mice and develop joint contractures and kyphosis leading to abnormal breathing patterns. They show difficulties walking and have an abnormal posture of the hindlimbs as they are not able to spread them like *mdx* or wild type mice (Figure 13). Mice die prematurely between 4 and 20 weeks. Only 50% is still alive at the age of eight weeks, and they rarely survive 12 weeks. Life span can be slightly extended by feeding the mice wet food or sunflower seeds, but it never exceeds 20 weeks. The primary cause of death is unknown, but is most often related to respiratory and heart failure combined with swallowing difficulties, so it might be generalised weakness and conditional loss.

Even though *mdx/utrn* $^{-/-}$ mice have a significantly reduced life span, muscle pathology does not dramatically differ from that observed in *mdx* mice. It is hypothesized that the absence of severe histopathology is caused by the lack of time for pathology to develop due to their short life span. The most dramatic difference in histopathology is seen in the extraocular muscles which are spared from pathology in *mdx* mice, but are severely affected in the *mdx/utrn* $^{-/-}$ mice, indicating that the upregulation of utrophin in particular prevents pathogenesis in *mdx* mice (Porter et al. 1998).

Figure 13. Phenotypical characteristics of *mdx/utrn* $^{-/-}$ mice.
A. Pictures of a C57BL/10ScSnJ mouse which is able to spread its hindlimbs upon handling by the tail and which does not show any malformations of the back. **B**. The *mdx/utrn* $^{-/-}$ mouse is unable to spread it hindlimbs normally as they contract upon handling. In addition, severe kyphosis is visible.

Subtle differences are seen in the onset of degeneration and development of necrosis which is already observed in six day old *mdx/utrn* $^{-/-}$ mice whereas at that time this is not yet observed in *mdx* mice. At the age of three weeks, when repeated cycles of degeneration and regeneration start in *mdx* mice, both strains have similar amounts of fibrosis, necrosis and inflammation. Although pathology in skeletal muscle but not diaphragm subsides in older *mdx* mice, this does not occur in *mdx/utrn* $^{-/-}$ mice, resulting in more intensive fibrosis and necrosis in 10 week old mice. Nevertheless, severity of histopathology at time of death is significantly less

compared to that seen in 18 months old *mdx* mice. Contrastingly, severity of the diaphragm is indistinguishable between the two models. In several muscles of *mdx/utrn* $^{-/-}$ mice fiber types tend to shift towards type I fibers. Although *mdx/utrn* $^{-/-}$ mice are much smaller than *mdx* mice, relative body weight to muscle mass does not significantly differ. Muscles of *mdx/utrn* $^{-/-}$ mice also seem to have problems to mature. Normally, only regenerating and immature fibers express developmental proteins like embryonic myosin heavy chains (eMHC) and neural cell adhesion molecule (N-CAM) and lose this expression upon maturing. Surprisingly, in a substantial group of large calibre fibers in *mdx/utrn* $^{-/-}$ mice eMHC and N-CAM expression remains present in contrast to *mdx* and wild type mice (Deconinck et al. 1997b;Deconinck et al. 1998;Grady et al. 1997b;Rafael et al. 1998).

With minor pathological changes of the NMJ in *utrn* $^{-/-}$ mice, extensive research has been carried out on the NMJ of *mdx/utrn* $^{-/-}$ mice. The axon of the synaptic terminal of the NMJ is similar to that of *mdx* mice, however, it almost completely lacks folding in the postsynaptic motor end plate regions. As previously mentioned, the synapse end plate of *utrn* $^{-/-}$ mice is identical to wild type mice, whereas a proportion of those seen in *mdx* mice are broken up to some extent and not as continuous. All synapses of *mdx/utrn* $^{-/-}$ mice are broken up into multiple boutons. No differences have been observed in intensities of AChRs detected by α-bungarotoxin staining between *mdx* and *mdx/utrn* $^{-/-}$ mice (Deconinck et al. 1997b;Grady et al. 1997b;van Putten et al. 2012). Like in the NMJ of *mdx/utrn* $^{-/-}$ mice the MTJ has significantly less foldings compared to *mdx* mice, which might be detrimental to force transmission. This causes marked increases in forces placed on individual contact areas between fiber membrane and the connective tissue matrix of the tendon resulting in membrane damage in these regions. A causative defect from nerves or synapses was ruled out after an experiment demonstrated that muscles that were repetitively stimulated had a similar time for tension to fall 50% as wild type mice, indicating that the impaired muscle function solely has a muscular basis (Grady et al. 1997b;Deconinck et al. 1997b).

In *mdx/utrn* $^{-/-}$ mice, the synaptic DGC complex is partly maintained despite the lack of both utrophin and dystrophin. This strengthened the observation that dystrophin expression is not upregulated in utrophin negative synapses. In *mdx/utrn* $^{-/-}$ mice levels of β-dystroglycan and α-sarcoglycans are comparable to those of *mdx* mice, while β_2-syntrophin and dystrobrevin are nearly undetectable. Even though expression of utrophin, dystrophin and a majority of the synaptic DGC proteins is altered in *mdx/utrn* $^{-/-}$ mice, expression of laminin-β2, agrin and rapsyn is unaffected. This indicates that synaptic development does not depend on these proteins, but that structural stabilization and maintenance do (Deconinck et al. 1997b;Grady et al. 1997b).

Muscle force is also more severely impaired in *mdx/utrn* $^{-/-}$ mice compared to *mdx* mice. *In vitro* electrophysiology showed that twitch tension is significantly reduced in steromastoid muscle, EDL, soleus and diaphragm. Relaxation time was also found to be greatly prolonged especially in the diaphragm. Time to peak tension, on the other hand, does not differ between *mdx/utrn* $^{-/-}$ and *mdx* mice in the steromastoid muscle, EDL, soleus and diaphragm. Interestingly, although force is greatly reduced in *mdx/utrn* $^{-/-}$ mice, repeated stimulation of the soleus did result in the same level of fatigue compared to *mdx* and wild type muscle, as force remained relatively stable. Apparently, where 40-50% of the soleus consists of fatigable type II fibers in *mdx* and wild type mice, in *mdx/utrn* $^{-/-}$ mice the soleus mainly consists of type I fibers (Deconinck et al. 1998;Grady et al. 1997b). The drop in force described can be partly addressed by administration of several compounds (Call et al. 2011;Yue et al. 2006).

Heart function of *mdx/utrn* $^{-/-}$ mice has been studied both by ECG and cine-MRI analysis. Before the age of five weeks, no visual abnormalities are present in cardiomyocytes.

From the age of seven weeks onwards, Evans blue dye uptake is significantly elevated and large patches of degenerating cardiomyocytes, inflammation and fibrosis has been reported in some studies (Chun et al. 2012;Hainsey et al. 2003;Verhaart et al. 2011;Grady et al. 1997b). Other studies did not find histopathology in 10 week old mice (Deconinck et al. 1997b). The onset of cardiomyopathy in *mdx/utrn* $^{-/-}$ is significantly earlier than that in *mdx* mice as first abnormalities are already observed at the age of five weeks consisting of a significantly decreased heart rate. Discrepancy in literature exists about the heart rate in eight week old mice as both a decrease and increase in heart rate has been described. Abnormal ECG patterns have been found with significantly decreased S- to R-wave ratios and depressed contractile function of the right ventricular muscles (Bia et al. 1999;Chun et al. 2012;Janssen et al. 2005). In depth cine-MRI revealed a diminished left ventricular function with a significantly decreased cardiac output, stroke volume, end diastolic volume and cardiac mass while ejection fraction remained comparable to age-matched wild type mice. These findings correspond to cardiomyopathy seen in DMD patients which also display a decreased stroke volume, resulting from hypertrophy of the left ventricle (Maciver and Townsend 2008). With declining heart function one would expect an increase in end diastolic volume, however, in *mdx/utrn* $^{-/-}$ mice the end diastolic volume is decreased probably due to the decreased cardiac mass. The right ventricular function of *mdx/utrn* $^{-/-}$ mice is less severely affected, with only a decreased ejection fraction. This probably results from their severe respiratory impairment which decreases the work load for the right ventricle, but to compensate for the low oxygen supply increases the work load for the left ventricle (Chun et al. 2012;Verhaart et al. 2011). With ECG, decreased thickness of the left ventricular posterior wall and intraventricular septum was found in 10 week old *mdx/utrn* $^{-/-}$ mice. The decreased ejection fraction and end diastolic volume seen already in eight week old mice with cine-MRI was observed by ECG in 15 weeks old mice, accompanied by end systolic volume and fractional shortening. This difference probably reflects the difference in sensitivity between the two techniques used.

1.2.5. The *mdx/utrn* $^{+/-}$ mouse

Only recently, more attention has been drawn to the *mdx/utrn* $^{+/-}$ mouse (Huang et al. 2011;Zhou et al. 2008;Rafael-Fortney et al. 2011;Verhaart et al. 2011;van Putten et al. 2012). Previously, this mouse model was only used for breeding purposes to obtain *mdx/utrn* $^{-/-}$ mice. A limitation of the latter model is the short life span making long-term experiments impossible. The *mdx/utrn* $^{+/-}$ mouse expresses utrophin from only one allele and has a life span comparable to that of *mdx* mice. It was postulated that the phenotype of *mdx/utrn* $^{+/-}$ mice would be more severe than that of *mdx* mice and therefore would mimic the human phenotype better, without premature death.

Zhou et al. described that the quadriceps and diaphragm of three and six months old *mdx/utrn* $^{+/-}$ mice had more pronounced inflammation and fibrosis respectively, compared to age-matched *mdx* mice (Zhou et al. 2008). The diaphragm was more severely affected than the quadriceps for both strains. This results in impairment of respiratory function at the age of three and six months in both strains, measured with whole body pleismography (method to measure respiratory rate and amplitude in conscious mice) (Huang et al. 2011). Only at the later time point, *mdx/utrn* $^{+/-}$ mice performed significantly worse than *mdx* mice. Our own study addressed functional performance of these mice and directly compared it to that of *mdx/utrn* $^{+/+}$ and $^{-/-}$ mice, revealing severely affected motor function (Chapter 3). Heart function of both 2, 5, 6 and 10 months old *mdx/utrn* $^{+/-}$ mice is however not more severely impaired than that of age-matched *mdx* mice, as both strains show a mild decrease in left ventricle function and a large decrease in

right ventricle function at the latter time point (Verhaart et al. 2011;Rafael-Fortney et al. 2011). Further research is needed to elucidate why the heart is spared in these mice. It might be that this is caused due to differences in physical abilities, causing less strain on the heart of *mdx/utrn* $^{+/-}$ mice, or due to differences in genetic background.

The first article in which the phenotype of *mdx/utrn* $^{+/-}$ mice was partly corrected by compound administration was published by Rafael-Fortney et al. They showed that *ex vivo* function of cardiac, limb and diaphragm was partly corrected by lisinopril and spironolactone administration starting at four or eight weeks of age (Rafael-Fortney et al. 2011). Also tetanic force of the EDL and diaphragm was significantly impaired in 20 week old *mdx/utrn* $^{+/-}$ mice compared to wild type mice. Direct comparison with *mdx* mice is impossible as these were not included.

As functional compensation for dystrophin by monoallelic expression of utrophin seems to be insufficient in *mdx/utrn* $^{+/-}$ mice, AON treatment was assumed to have a more pronounced effect in these mice compared to *mdx* mice. Upon subcutaneous administration of 2OMePS for six months, we observed that AON uptake, exon skip levels and functional improvement was significantly higher in *mdx/utrn* $^{+/-}$ than in *mdx* mice (Tanganika-de Winter et al. manuscript submitted).

Based on these studies, it can be concluded that the *mdx/utrn* $^{+/-}$ mouse is a more severely affected model. This suggests that the functional compensation of dystrophin by heterozygous expression of utrophin is incomplete. Taken together, this underlines that the *mdx/utrn* $^{+/-}$ mouse is a better model than the *mdx* or *mdx/utrn* $^{-/-}$ mouse for long term experiments.

1.3. Low dystrophin levels in human and mice

1.3.1. DMD and BMD carriers

Although no therapy is available for DMD yet, different potential therapeutic approaches aiming to restore dystrophin synthesis are currently tested in clinical trials. These trials result in the expression of low dystrophin levels. However, it is not yet known how these levels affect disease pathology and which levels are needed to maintain or improve muscle integrity, to prevent against exercise-induced damage or to improve muscle function. In addition, it is unknown whether the percentage of dystrophin that is needed for these outcome measures will be similar for skeletal muscle and heart, or whether different muscles need different levels.

The first hints to answer these questions were obtained from DMD and BMD carriers. Symptoms in these females vary from mild muscle pain and cramps, to severe muscle weakness leading to wheelchair dependency. Muscle weakness is proximally distributed first affecting the legs and later the shoulder girdle. The age at onset ranges from the first to the fourth decade. Generally, onset before the age of 15 results in a severe phenotype (Hoogerwaard et al. 1999). The majority of DMD and BMD carriers (76% and 81% respectively) express ~50% of dystrophin early in life, based on random X-inactivation levels and these females are not affected. This indicates that these levels are sufficient to maintain skeletal muscle function and prevent pathology (Pegoraro et al. 1995;Schmidt-Achert et al. 1993). Non-random X-inactivation results in a mild dystrophic phenotype in rare cases. Despite muscle weakness being absent or only very mild, a small percentage (~8%) of the carriers develops DMD-associated dilated cardiomyopathy (Ogata et al. 2000;Hoogerwaard et al. 1999).

Manifesting carriers have also been described which express <50% of dystrophin. The prevalence of clinically manifesting DMD and BMD carriers in the female population is 1:45,000 and 1:100,000 respectively. Several mechanisms are known to cause symptoms in these carriers. The majority of manifesting carriers are the consequence of unfortunate, skewed X-inactivation (section 1.3.4.1.). In this case, the intact X-chromosome is predominantly inactivated, so that the X-chromosome with the *DMD* mutation is active in the majority of the cells. Disease severity in these carriers depends on the degree of inactivation of the intact X-chromosome. Examinations of biopsies from carriers reveal a mosaic pattern of fibers that do express dystrophin at normal intensities and fibers that lack dystrophin expression (Azofeifa et al. 1995;Pegoraro et al. 1995;Soltanzadeh et al. 2010). Some manifesting carriers however, have gross chromosomal rearrangements involving translocations between the X-chromosome and an autosome. These translocations lead to almost complete inactivation of the normal X-chromosome with the intact *DMD* gene, resulting in much decreased dystrophin levels (Lindenbaum et al. 1979;Boyd et al. 1986). Alternatively, a few rare cases have been described of females who suffered from Turner's syndrome (patients with this syndrome lack one X-chromosome) and also carried mutations in their *DMD* gene. In these patients, lack of dystrophin resulted in the typical DMD phenotype (Ferrier et al. 1965;Bjerglund and Nielsen 1984;Chelly et al. 1986). Also a number of monozygotic twins have been described with heterozygous mutations in their *DMD* gene. In all these cases one of the twins was phenotypically normal while the other had severe DMD-like symptoms. The affected twin showed unfortunate skewed X-inactivation resulting in low dystrophin levels. It is hypothesized that the twinning process directly relates to the observed low dystrophin levels, as no reports exists on cases in which both twins are manifesting. In rare occasions, during random X-inactivation, the maternal derived X-chromosome (Xm) is inactivated in particular clumps of cells while the paternal derived X-chromosome (Xp) is inactivated in other clumps. These clumps

might define each other as 'foreign' which initiates them to separate 3-8 days post fertilization (Richards et al. 1990). One article also reported a twin in which the unaffected girl had random X-inactivation while the affected girl had unfortunate skewed X-inactivation. This resulted from asymmetric splitting of the inner cell mass (ICM) (Lupski et al. 1991).

1.3.2. BMD patients

As mentioned in section 1.1.4., BMD patients express low levels of truncated but partly functional dystrophin. In these patients, disease severity varies from very mild, in which patients remain asymptomatic until later in life, till quite severe where patients are diagnosed in childhood and lose ambulation in the early to late teens. The clinical outcome depends primarily on the amount of dystrophin expressed. Patients expressing <3% of normal on average become wheelchair dependent before the age of 11 years. Levels between 3 and 10% lead to wheelchair dependence between the age of 13 and 20 years whereas levels >20% delay wheelchair dependence till the second decade (Hoffman et al. 1988;Hoffman et al. 1989). Most patients lose ambulation between 20-30 years after diagnosis. Life span of mildly affected patients is near normal, whereas severely affected patients die between the age of 40 and 50 years. Some BMD patients also suffer from dilated cardiomyopathy, which can be the main symptom in the less severely affected patients. Other patients only have very mild symptoms of either skeletal muscles and/or heart (Helderman-van den Enden et al. 2010). A case report of one BMD patient expressing 29% of dystrophin in a uniform manner revealed that this already completely prevented muscle pathology (Neri et al. 2007). Another study described patients expressing <10% dystrophin that were more severely affected than the patient that expressed ~20% of dystrophin (Beggs et al. 1991). Taken together, expression of dystrophin correlates with disease severity and even levels of ~30% can largely prevent pathogenesis.

1.3.3. Mouse models expressing low dystrophin levels from birth

With only limited access to tissues from DMD and BMD carriers and BMD patients, in-depth research was warranted in animal models expressing low dystrophin levels. Experiments in heterozygous *mdx* mice revealed that also in mice ~50% of dystrophin completely prevents skeletal muscle pathology. Additionally, they revealed that the number of dystrophin positive fibers increases over time due to their survival advantage over dystrophin negative ones. Surprisingly, these mice do not develop any heart pathology, while this is observed in ~8% of the DMD and BMD carriers. The cause for this difference is poorly understood (Bostick et al. 2008;Tanaka et al. 1990).

From the early nineties onwards, transgenic mice expressing full-length or truncated dystrophin of murine or human origin were generated to study the applicability of gene therapy for DMD (Dunant et al. 2003;Lee et al. 1993;Phelps et al. 1995;Rafael et al. 1994;Wells et al. 1995). The majority of these lines expressed dystrophin at intensities exceeding wild type levels or at both moderate and high intensities. Interestingly, some of these mice expressed <50% dystrophin as assessed by Western blot in a uniform or mosaic manner (Table 4). The way in which dystrophin was expressed and at which intensities differed per line. Within an individual mouse differences in expression between muscles and/or fiber types were observed, with fast fibers predominantly expressing dystrophin (Lee et al. 1993). These differences resulted most likely from the autosomal location of the transgene and the promoter by which it is driven.

Studies in these transgenic mice indicate that the beneficial effect of different types of dystrophins (full-length versus truncated) and the manner in which it is expressed (uniform versus mosaic) varies. Complete restoration of disease pathology was observed in mice uniformly expressing full-length dystrophin (mouse line 852 diaphragm) at intensities of ~20% of wild type levels. Expression of 40% of truncated dystrophin (mouse line 12157 quadriceps) did not completely restore pathology, although it dramatically reduced symptoms. This was confirmed by others: an incomplete restoration of pathology was observed upon uniform expression of 20-30% of truncated dystrophin (lacking exon 17-48), while no pathology was seen in mice expressing similar amounts of full-length dystrophin (Wells et al. 1995). This suggests that fibers expressing truncated dystrophin are more vulnerable to damage than those expressing full-length dystrophin (Chamberlain 1997;Phelps et al. 1995;Wells et al. 1995).

Author	Transgenic model	Dystrophin pattern	Histopathology
Lee 1993	Full-length murine	Mosaic (only dys positive in fast fibers) Western blot 20% in 1 month while 60% in 4 month old mice	Improved
Rafael 1994	Truncated murine lack 71-74	Mosaic 50% dys positive fibers in Qua (intensities from 1 to >100%) 10-20% dys positive fibers in Dia	Qua: improved fibrosis Dia: no improvement
Phelps 1995	Full-length murine Line 8487	Mosaic Western blot 15% dys in Qua Western blot <5% dys in Dia	Qua: partial reduction CN Dia: reduction fibrosis and inflammation
Phelps 1995	Full-length murine Line 852	Uniform (U)/Slightly variable (Sv) Western blot >70% dys in Qua (U) Western blot 20% dys in Dia (Sv)	Qua: prevented all pathology Dia: prevented all pathology
Phelps 1995	Truncated murine lack 17-48 Line 12157	Uniform (U)/Mosaic (M) Western blot 40% dys in Qua (U) Western blot 20% dys in Dia (M)	Qua: dramatic reduction of pathology Dia: no improvement
Wells 1995	Human full-length	Uniform Western blot 20-30% dys in Dia	Prevented all pathology
Wells 1995	Human mini-dys lack 17-48	Uniform Western blot 20-30% dys in Dia	Nearly prevented all pathology still some CNs
Hauser 1997	MCK promoter driven expression	Uniform Western blot 20% of wild-type in Dia	Nearly prevented all pathology
Hauser 1997	MCK promoter driven expression	Mosaic Levels not mentioned in article	Improvement depended on % dys positive fibers
Dunant 2003	MCK promoter driven expression	Mosaic (only dys positive in fast fibers) In ~50% of the fibers	Improved
Stillwell 2009	Wild-type ES-cell incorporation	Mosaic Western blot 60-100% or <5% of wild-type	Dose dependent improvement
Li 2008	*Mdx*^{3cv} mouse	Uniform Western blot ~5% of wild-type	Some improvement in young not old mice

Table 4. Overview of *mdx* mice generated that express <50% dystrophin.
This table summarizes some of the transgenic *mdx* mice that express low levels of full-length or truncated dystrophin from murine or human origin. Dystrophin expression is either in a mosaic or uniform manner. The amount of dystrophin expressed correlates with histopathology. CN= centralized nuclei, Dia= diaphragm, Qua= quadriceps.

Mosaic expression of dystrophin clearly protects fibers to damage to a smaller extent than homogenous expression, as higher total protein levels are needed to prevent pathology. While full-length dystrophin expressed at 20% of wild type uniformly, completely prevented pathology

(as stated above), mosaic expression only partly decreased the percentage of centralized nuclei (line 8487). However, mosaic expression of 20% of truncated dystrophin (line 12157), did not improve histopathology at all (Phelps et al. 1995). This indicates that the uniformity of dystrophin expression might be more relevant than the level of expression in protecting muscle fibers against pathogenesis. This observation was confirmed in an independent study generating different transgenic mouse lines (Hauser et al. 1997).

Although decreases in numbers of centralized nuclei were found in the majority of these lines, no clear correlation was observed between dystrophin expression in a particular fiber and the presence of nuclei located at the periphery or the center of that fiber (Rafael et al. 1994). However, others observed that dystrophin negative fibers neighbouring dystrophin positive ones were more likely to have nuclei at the periphery, than those surrounded by dystrophin negative fibers (Dunant et al. 2003). An increment in dystrophin positive fibers over time, which was observed in heterozygous *mdx* mice, was found in some (Lee et al. 1993), but not all transgenic models (Dunant et al. 2003;Rafael et al. 1994). This might be caused by the different ways in which these models were generated, or due to the young age of the mice at time of assessment.

Besides transgenic mice, alternative approaches have also been undertaken to generate mice expressing low dystrophin levels. Stillwell et al. injected wild type ES cells into *mdx* blastocytes (Stillwell et al. 2009). Depending on the incorporation of the ES cells, mice expressed dystrophin in either a very high (60-100%) or low (<5%) percentage of the muscle fibers at wild type intensities. The percentage of dystrophin positive fibers in these mice also differed per muscle. A dose-dependent restoration of muscle pathology was observed. This approach of generating animals for further investigations is less favourable as it is labour intensive and results in mice with dystrophin levels on both extremes of the scale only.

The final model expressing very low dystrophin levels is the *mdx*^{3cv} mouse. As described earlier, these mice express dystrophin in all fibers but at ~5% of the intensity of wild type mice. Li et al. observed that these levels resulted in some improvements in young but not in older mice. The EDL of young mice was partially protected from eccentric contraction-induced injury and had a significant higher tetanic force compared to *mdx*^{4cv} mice (Li et al. 2008). Also the forelimb grip strength of the *mdx*^{3cv} mice was slightly increased. No difference in CK was detected, nor did histopathology differ between *mdx*^{3cv} and ^{4cv} mice.

1.3.4. Treated *mdx* mice expressing low dystrophin levels

Despite the lack of a good mouse model to assess the effect of low dystrophin levels on disease pathology, knowledge could still be obtained from mice that expressed low dystrophin levels upon treatment with AONs, AAV-U1 and gentamycin. These studies primarily focussed on the effect of low dystrophin levels on functional and biomarker outcome measures. Intramuscular PMO administration revealed that dystrophin expression in ~20% of the fibers (resembling ~10% assessed by Western blot) largely protects muscles against eccentric contraction induced injury. The functional improvement correlated more strongly to the number of dystrophin positive fibers than to levels assessed by Western blot, which again indicates that the total number of fibers expressing dystrophin is most relevant (Sharp et al. 2011). The same compound was also systemically injected in *mdx* mice at a low (5mg/kg) and high (50mg/kg) dose for 20 or 50 weeks. Short term treatment resulted in 23% (5mg/kg, resembling 20% on Western blot) and 27% (50mg/kg, 40% on Western blot) of dystrophin positive fibers in the tibialis anterior, expressing dystrophin at intensities slightly lower and higher than wild type for the low and high dose respectively. This resulted in improved grip strength and resistance to eccentric contractions.

Treatment for 50 weeks with the same doses resulting in ~60% of dystrophin in the tibialis anterior improved voluntary activities and grip strength, but not resistance to eccentric contractions. Histopathology in all mice was only slightly improved (Malerba et al. 2011b). Uniform dystrophin at intensities of 20% of wild type, induced by gentamycin treatment has been found to partly protect muscles even while chronically challenged with horizontal treadmill exercise twice weekly. In these mice, histopathology and CK levels were reduced, however higher levels were needed to restore altered calcium homeostasis (De Luca et al. 2008). Very low dystrophin levels (<10%) resulting from exon skipping either induced with 2OMePS or AAV-U1 have been shown to reduce the expression of some mRNA and miRNAs involved in various aspects of disease pathology (Verhaart et al. 2012;Cacchiarelli et al. 2010).

1.3.5. The *mdx-Xist*$^{\Delta hs}$ mouse

Despite the fact that transgenic mice and mice treated with potential therapeutic compounds provided us with important information regarding the effects of low dystrophin expression on muscle pathology, these approaches are not ideal for more in-depth research. The disadvantages of the transgenic lines are the big differences in dystrophin intensities between individual fibers as well as fiber type specific dystrophin expression which are not favoured. An obvious disadvantage of treating mice is that treatment is quite expensive, stressful to the mice and labour intensive. With this in mind, we generated the *mdx-Xist*$^{\Delta hs}$ mouse model, which expresses low levels of dystrophin from birth onwards based on intentionally skewed X-inactivation.

1.3.5.1. X-inactivation

In all animals in which there is an imbalance in the amount of sex-chromosomes (e.g. female humans and mice carry two X-chromosomes, while males only carry one X-chromosome), compensation is ensured by sex chromosome inactivation (generally X-inactivation in mammals) resulting in equal transcript levels between females and males (Lyon 1961). This is a critical event as failure results in significant copy number variation of around 1000 genes resulting in embryonic lethality or malformations. Although X-inactivation was discovered 50 years ago, the exact mechanism, which differs between species, is still poorly understood. Two distinct cycles of X-inactivation (imprinting and random X-inactivation) have been described in mice, whereas only the latter occurs in humans. In mice, at the 2-4 cell stage, equal levels of both the Xp and the Xm are active (Figure 14). From this stage onwards, Xp is inactivated via imprinting, ensuring Xm being active in all extra-embryonic tissues. Maternal germ line cells are protected against inactivation by an imprint which represses *Xist* expression (see below). The inactive state of Xp is reversed again in the ICM of the blastocytes. Thereafter, either Xp or Xm is inactivated in each cell during random X-inactivation. All descendants of these cells inherit the same inactivation pattern which is maintained throughout life. Only in the female germ line, the inactivation pattern is reversed ensuring that all oocytes have an active X-chromosome (Xa) (Ng et al. 2007).

Both imprinted and random X-inactivation rely on one single locus; the X-inactivation center (Xic). The Xic expresses many regulatory elements which mediate in the inactivation process. At the onset of random X-inactivation, the X-pairing region ensures pairing of the X-chromosomes. Subsequently, the number of X-chromosomes rerlative to the number of autosome is counted. This is done based on levels of *Rnf12*, which is expressed from the Xic.

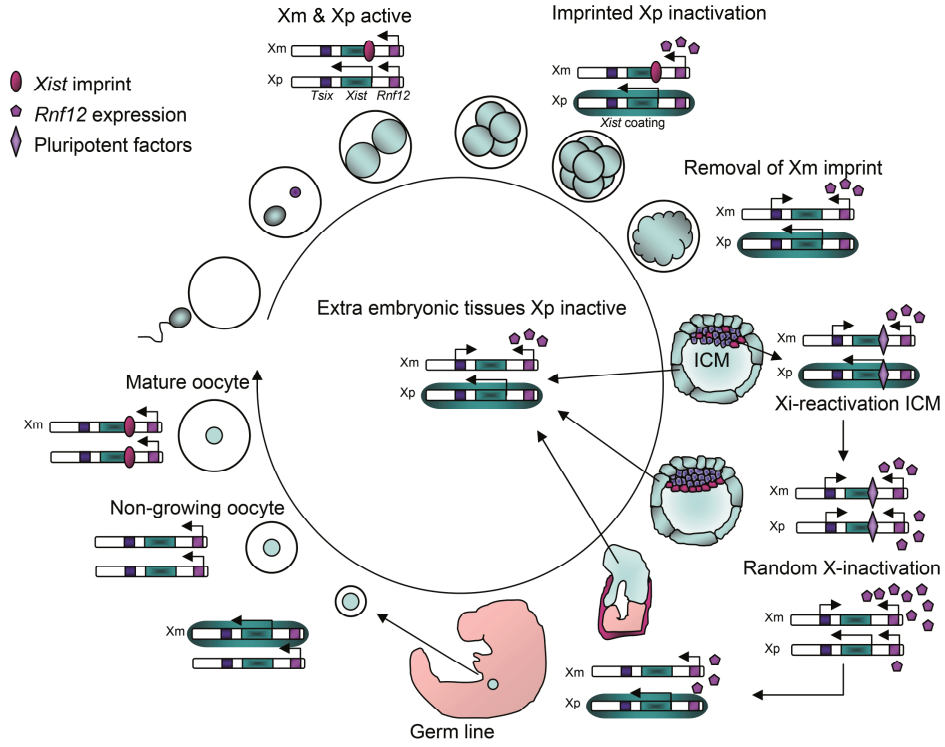

Figure 14. The mechanism of random X-inactivation in mice.
In mice the paternally derived X-chromosome (Xp) is inactivated in all extra-embryonic tissue from the 2-4 cell stage onwards. The maternally derived X-chromosome (Xm) is protected from X-inactivation by an imprint. In the blastocytes, upon reversion of the inactive state of the Xp, either the Xp or Xm are inactivated in a random manner. At initiation of random X-inactivation both Xp and Xm express high levels of *Rnf12*, *Tsix* and pluripotency factors. In one of the two chromosomes, *Rnf12* and *Tsix* expression decrease initiating overexpression of *Xist* on the other X-chromosome. The *Xist* expression leads to coating of that X-chromosome which makes it transcriptional inactive. The active or inactive state of the X-chromosomes is maintained throughout life. Only the X-chromosomes in the germ line remain active and become imprinted (Picture based on by Augui et al 2011 Nat. Rev. Genet.).

Females express twice as much *Rnf12* compared to males. Regardless of the number of X-chromosomes present, only one of them remains active. This decision is made during an interplay between the main players *Rnf12*, *Tsix*, *Jpx* and *Xist*, but the pluripotency factors NANOG, OCT4 and SOX2 are thought to play a role as well (Augui et al. 2011). *Xist* and *Tsix* are two long non-coding RNAs which are expressed from partly the same location of the Xic in sense and antisense direction respectively. At initiation of X-inactivation, both X-chromosomes express *Rnf12* and *Tsix* and thereby trigger the expression of *Xist*. Later on, downregulation of *Rnf12* and *Tsix*, and upregulation of *Jpx* on the future inactive X-chromosome (Xi) lead to a monoallelic upregulation of *Xist* (Tian et al. 2010;Lee et al. 1999). This results in coating of this X-chromosome, initiating its inactivation. Consequently, Polycomb protein complexes are recruited which ensure packaging of the DNA by histone modifications into heterochromatin thereby making it transcriptionally inert. In this way, a discrete body in the nucleus called the Barr body is formed. As previously mentioned the inactive state of Xi is inherited by daughter cells and maintained throughout life. Some regions located on the short arm of the X-chromosome, escape inactivation.

These regions are called pseudoautosomal regions and contain genes that are also present on the Y-chromosome, obviating the need for dosage compensation (Carrel and Willard 2005).

To study the mechanism of X-inactivation, many mouse models have been generated each lacking an important modulator of X-inactivation on one or both alleles (Barakat et al. 2011;Shin et al. 2010;Tian et al. 2010;Penny et al. 1996). We used one of these models (*Xist*$^{\Delta hs}$ mouse) for the generation of two new innovative mouse models for DMD, which are described in Chapters 5, 6 and 7 of this thesis. As previously mentioned, in these models the phenomenon of skewed X-inactivation, as seen in some female symptomatic DMD and BMD carriers, was used as a concept. The mouse model used had a PGKneo cassette inserted immediately upstream of the *Xist* promoter P_1 (Newall et al. 2001). The authors observed that in heterozygous *Xist*$^{\Delta hs}$ females, targeting this locus resulted in preferential inactivation in ~80-90% of X-chromosomes carrying the mutation in *Xist*. We crossed *Xist*$^{\Delta hs}$ females with *mdx* males in our lab. In the female pups, the mutated *Xist* gene was heterozygously expressed, resulting in preferential inactivation of the X-chromosome with the mutation in the *Xist* gene. As these X-chromosomes do not carry a mutated *Dmd* gene, their preferential inactivation causes a preponderance of active X-chromosomes from the *mdx*-background on overall deficit of dystrophin positive cells in female progeny. Therefore, female *mdx-Xist*$^{\Delta hs}$ offspring typically express dystrophin levels between 3-47% depending on their X-inactivation ratio. Detailed information regarding their phenotype can be found in Chapters 5 and 6 of this thesis.

1.3.6. The *mdx/utrn* $^{-/-}$ */Xist*$^{\Delta hs}$ mouse

In *mdx* mice utrophin very effectively compensates for the lack of dystrophin resulting in a very mild phenotype. It is therefore of interest to study the effects of low dystrophin levels in a utrophin negative background. Due to the severe phenotype of *mdx/utrn* $^{-/-}$ mice, this model is more suitable to assess the dystrophin levels needed for improved life expectancy as well as pathology and muscle function.

Several labs have put effort in generating such a mouse over time, unfortunately without any success as none of the models expressed a variety of low dystrophin levels. The first attempt was made in 1999, in a paper focussing on the role of dystrophin and utrophin in non-muscle tissues but no protective effects were observed for the low dystrophin levels expressed (Rafael et al. 1999). Several years later, Li et al. generated utrophin negative *mdx*^{3cv} mice (Li et al. 2010). For these mice, a significantly improved life span has been reported (in contrast to the findings of Rafael et al). The difference might result from differences in backgrounds of the strains among others.

Exploiting the principle of skewed X-inactivation patterns like we did for the *mdx-Xist*$^{\Delta hs}$ mice, we generated *mdx/utrn* $^{-/-}$ mice expressing low dystrophin levels. To utilize these mice, *utrn* $^{-/-}$ *Xist*$^{\Delta hs}$ males were needed. These mice were generated by crossing *Xist*$^{\Delta hs}$ females with *utrn* $^{-/-}$ *hDMD* $^{+/-}$ males. The *hDMD* mouse has an intact and functional copy of the human dystrophin gene on a C57BL/6 background. This mouse model was generated earlier in our group ('t Hoen et al. 2008). The *hDMD* gene functionally compensates for the absence of mouse dystrophin. In the pups we selected against the *hDMD* gene so that we obtained *utrn* $^{-/-}$ *Xist*$^{\Delta hs}$ mice. These mice were further crossed with *mdx/utrn* $^{+/-}$ females to generate *mdx/utrn* $^{-/-}$ */Xist*$^{\Delta hs}$ female pups. This model is the first in its kind expressing dystrophin levels that are between 1 and 38% and extensive research is described in Chapter 7 of this thesis.

1.4. Outcome measures

1.4.1. Functional tests

Preventing or delaying the onset of progressive loss of muscle function is the ultimate goal of clinical trials currently ongoing for DMD. Therefore, muscle function is the most important outcome measure in pre-clinical screening of potential therapeutic approaches and compounds. To determine motor function pre-clinically in mouse models of DMD, several different functional tests have been designed. As they do not interfere with disease progression, they can be used to either assess the course of natural history of the disease, or the effects of compounds on disease progression (Chapter 2) (van Putten et al. 2010). Examples of non-invasive functional tests are the grip strength, the rotarod and hang tests (Figure 15A-E). Using the grip strength test, strength of either the forelimbs or hindlimbs can be tested based on the instinct of a mouse to grasp an object (Connolly et al. 2001). The rotarod is used to test muscle function and coordination and involves walking on a rotating tube that increases in speed in the first minute (Chapillon et al. 1998). Balance, coordination and muscle condition can be tested with hanging tests. A distinction can be made between two types of hanging tests in which either only the forelimbs of all four limbs are used at start of the test. The start position with two limbs allows direct distinction in the functional abilities of a mouse to also start using its hindlimbs and tail thereby reducing the maximum load per leg. Contrastingly, in the hang test in which all limbs are used from the start onwards equal chances are given to all mice (Raymackers et al. 2003;van Putten et al. 2010). With dystrophin negative fibers being vulnerable to damage caused by exercise, the type, load and duration must be correctly chosen in these cases.

On the other hand, forced treadmill exercise can be chronically used to intentionally exacerbate disease progression and to determine the protective effect of compounds more thoroughly in *mdx* mice (Figure 15F). Horizontal treadmill running increases muscle necrosis of the quadriceps, gastrocnemius and triceps, whereas the diaphragm and tibialis anterior are affected to a lesser extent. Also an increase in the number of centrally nucleated fibers, the proportion of fast fibers and serum CK levels is found, whereas muscle strength decreases (De Luca et al. 2005;Payne et al. 2006;Radley et al. 2008;Pierno et al. 2007). Besides horizontal treadmill running, also downhill running can be applied. As *mdx* fibers are especially vulnerable to eccentric contractions, this type of exercise induces major pathology. Muscles mostly affected by this exercise are the diaphragm and triceps, while the tibialis anterior and EDL only show minor damage (Brussee et al. 1997). Alternatively, the treadmill can also be used to measure the ability of *mdx* mice to run on a horizontal treadmill and encouraged to run till exhaustion. Six months old *mdx* mice exhaust earlier (after ~12 min) than age-matched wild type mice (~after 60 min) (Brunelli et al. 2007;Minetti et al. 2006).

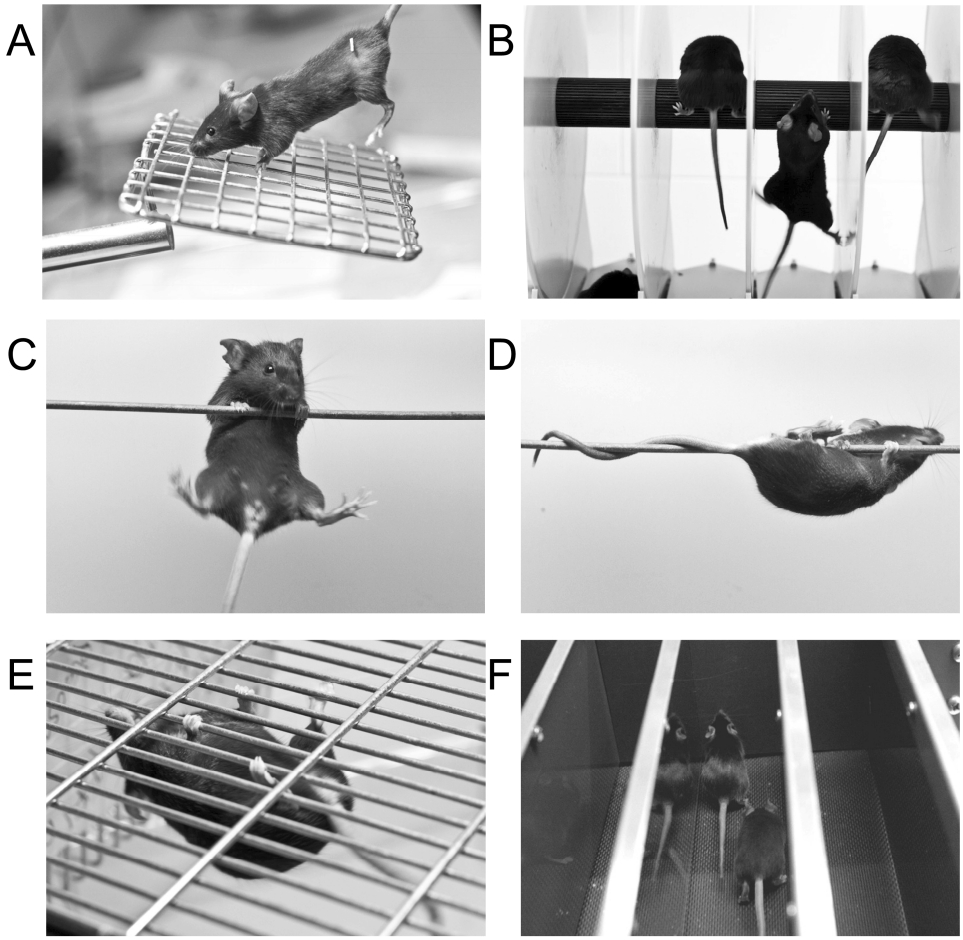

Figure 15. Overview of the most often used functional tests.
A. Grip strength device used to monitor strength of the extremities. **B**. Rotarod running device, used to measure the ability of a mouse to run on a rotating rod. **C-D**. Two limb hanging wire test. In this test, the begin position is with the two forelimbs. Mice that perform well can be distinguished by their ability to use their hindlimbs and tail additionally. **E**. Hanging wire test in which the start position is with four limbs. **F**. Treadmill device used in experiments to either exacerbate disease progression or to assess running abilities.

Interestingly, voluntary running exercise results in improved muscle function. Voluntary wheel running is assessed in mice that are individually housed in a cage enriched with a metal wheel and is used to determine neuromuscular impairment. Studies assessing the direct consequences of this exercise on muscle pathology in *mdx* mice showed that within 24-48 hours post exercise necrosis is doubled in the quadriceps, while the tibialis anterior remained spared. Also the EDL is more affected than the plantaris and soleus muscles (Archer et al. 2006;Radley and Grounds 2006). Long term voluntary running exercise has beneficial effects on muscle quality of *mdx* mice (Dupont-Versteegden et al. 1994;Carter et al. 1995;Landisch et al. 2008;Hara et al. 2002;Hayes and Williams 1996). Accumulation of dirt increases the resistance of the wheel rotation which is likely to influence outcomes, as even mild resistance already influences skeletal and heart muscle physiology in wild type mice (Konhilas et al. 2005). Interestingly, increased

workload does not negatively impact pathology in *mdx* mice. It does however force *mdx* mice to run less when the load is 13% of their body weight. This is only observed in wild type mice when the load is 25% of their body weight (Call et al. 2010). Alternatively voluntary activity can also be assessed in cages equipped with multiple photocell receptors and emitters that monitor horizontal and vertical movements (Spurney et al. 2009).

To summarize; major differences in the impact of different exercise types on disease pathology have been described ranging from extremely detrimental to beneficial. Generally, treadmill running is detrimental to *mdx* mice, voluntary exercise is beneficial and other functional tests do not have a distinct impact on muscle pathology. Exercise-induced histopathology does differ between muscles, as type II fibers are more prone to damage than type I fibers. Additionally, the likelihood that specific muscles get damaged depends on the recruitment of these muscles during the specific exercise. Also age influences the impact with young *mdx* mice being more vulnerable to exercise than old mice (Faist et al. 2001). When exercise is applied, physiological, metabolic and vascular adaptations can be observed (Kobayashi et al. 2008). It has been reported that these response can differ between dystrophic and wild type strains, which in turn might affect drug absorption and metabolism. A high degree of standardization in the methodology is essential to enable comparisons between experiments and labs. In a collaborative effort of the TREAT-NMD network of excellence and the Wellstone Center, numerous standard operating procedures for functional tests to be used in *mdx* mice are now available (http://www.treat-nmd.eu/resources/research-resources/dmd-sops/). Eventually extended knowledge on the influence of exercise on disease pathology is important to better advise DMD patients.

1.4.2. Heart function

In mice, heart function can be measured by ECG or MRI. During an ECG-scan, the heart's electric activities are recorded, which is visualised by waves and peaks (Figure 16). To do so, the mouse is anesthetized, after which two fine needle electrodes are subcutaneously inserted at the ventral junction between the chest and the right and left forelimbs. Additionally, one needle is inserted at the junction between the lower abdomen and left hindlimb (Bia et al. 1999). Recordings provide information regarding the heart rate, the rhythm of the heart beat and the strength and timing of the electrical signals. The cycle starts with spontaneous depolarization in the sinoatrial node located at the top of the right atrium, transmitting an electric signal that spreads from the right to the left atrium and results in contraction of the atria. The signal ends up in the atrioventricular node while the blood is pumped to the ventricles. This atrial depolarization is characterized in the ECG by the P-wave. The duration of this (PR interval) is an estimation for atrioventricular node function. The signal is further directed to the His bundle and the Purkinje cells. Both ventricles are depolarized when the signal is redirected back to the atria. This results in contraction (systole) of the ventricles pumping blood through the aorta and is reflected by the QRS complex. Relaxation of the atria and ventricles is ensured upon repolarisation of the ventricles (T-wave) which enables the heart to fill with blood (diastole). The QT interval reflects the de and repolarisation of the ventricles e.g. the time it takes for the ventricles to fully contract and relax. The ST segment is the period of depolarization of the ventricles (Bia et al. 1999;Hurst 1998).

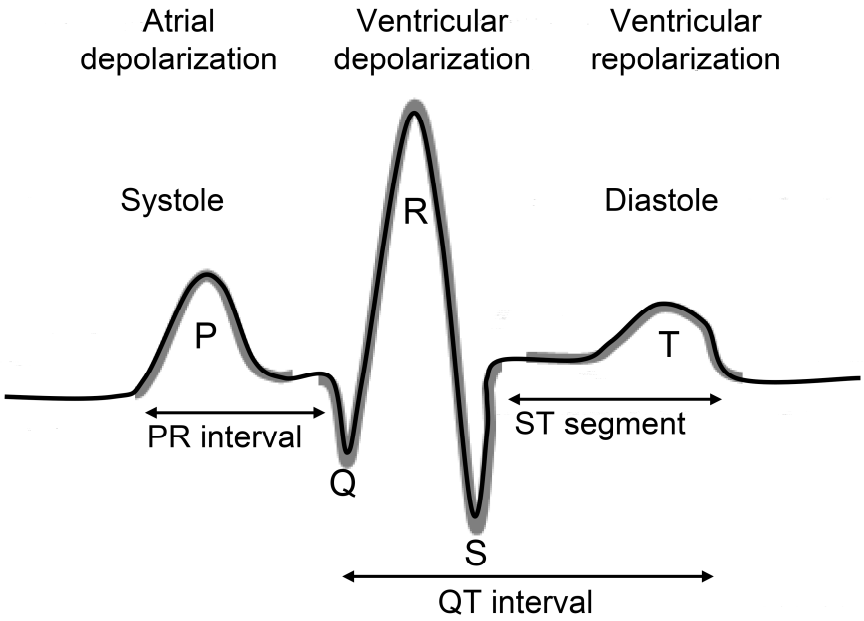

Figure 16. Electrocardiogram of the heart.
The ECG consists of a P-wave indicating atrial depolarisation, the QRS peak which resembles ventricular depolarisation whereas repolarisation of the ventricles is resembled by the T-wave. The PR interval reflects the time of the signal leaving the sinoatrial node to it ending up in the AV node. The QT interval is a reflection of the de and repolarization of the ventricles, so the total time for the ventricles to fully contract and relax. The ST segment is the period of depolarization of the ventricles. Heart failure is characterized by alterations in amplitude and timing of the waves and peaks.

The major disadvantage of the ECG is that it only provides indirect information regarding the ventricular contractions. Additionally, ECG measurements are significantly hampered in severely affected mouse models like the *mdx/utrn* $^{-/-}$ mice in which the position of the heart varies per individual due to severe kyphosis. Here, reliable data can still be obtained with MRI as this technique enables more in-depth and accurate assessments of the heart function (Verhaart et al. 2011). An MRI machine has an extremely powerful magnetic field, which forces all the hydrogen atoms in the body to align to the direction of this field. Upon generation of extremely strong radiofrequency waves, the nucleus of the hydrogen atoms in the body move slightly. When this is turned off, these atoms regain their position, sending out radiofrequency waves themselves which are detected and used to generate a picture. Hydrogen atom rich areas (i.e. blood) appear much brighter in these images then areas containing less hydrogen atoms (muscle) (Bothwell and Griffin 2011). Although mice are scanned in a vertical position in the coil of the MRI this does not affect heart function (Schneider et al. 2003). Pictures obtained cover the entire heart beat cycle and can be used to precisely determine contractions. The most often used outcomes measures are: the end diastolic volume and end systolic volume which represent the volume in the ventricle prior contraction and after ejection respectively. The stroke volume is the difference between those two parameters and represents the volume of blood which is pumped from a particular ventricle within a heart beat. The ejection fraction is the amount of blood which leaves the heart at every heart beat. The cardiac output is the volume of blood pumped by a particular ventricle within one minute (Crisp et al. 2011;Verhaart et al. 2011;Zhang et al. 2008).

1.4.3. Serum and gene biomarkers

Although functional tests are extremely valuable outcome measures, subtle changes cannot easily be detected. For potential upcoming therapies like AON-induced exon skipping, chronic administration will be necessary. Timing of these administrations will probably be patient dependent and monitoring disease progression with the use of serum biomarkers will be critical. Biomarkers are biological measurable parameters that offer a way to monitor normal and abnormal processes in e.g. body fluids that replace invasive biopsies (Nadarajah et al. 2011). One would aim for the use of robust biomarkers that are stable (not influenced by life style and dietary changes), specific (to a disease, pathway or genotype) and can repeatedly be quantified in which different analysis and laboratories obtain similar results. To date, serum CK has been used as a biomarker for diagnostic screenings of DMD patients. As CK leaks out of damaged muscle fibers, levels are low in more advanced stages of the disease when fibers are largely replaced by fibrotic and fat tissue. Additionally, CK levels increase upon activity, even in healthy controls. This reduces the utility of this biomarker, requiring the discovery of more robust biomarkers that can be used to monitor disease progression throughout the patient's life. In this thesis, several serum and gene expression biomarkers were assessed. To identify potential biomarkers, targeted (based on literature) and non-targeted (screening serum from DMD, BMD and controls to identify which proteins are differentially expressed) approaches were used for the gene and serum biomarkers respectively. The biomarkers used in this thesis were identified by the targeted approach and are important players in either maintenance of the ECM, inflammation, fibrosis, regeneration, heart and mitochondrial function.